The role of hyperpolarization-activated cationic current in spike-time precision and intrinsic resonance in cortical neurons in vitro

Philippe Gastrein, Emilie Campanac, Célia Gasselin, Robert H. Cudmore, Andrzej Bialowas, Edmond Carlier, Laure Fronzaroli-Molinieres, Norbert Ankri, Dominique Debanne

J Physiol 589.15 (2011) pp 3753–3773

The Journal of Physiology

The role of hyperpolarization-activated cationic current in spike-time precision and intrinsic resonance in cortical neurons *in vitro*

Philippe Gastrein[1,2], Émilie Campanac[1,2], Célia Gasselin[1,2], Robert H. Cudmore[1,2], Andrzej Bialowas[1,2], Edmond Carlier[1,2], Laure Fronzaroli-Molinieres[1,2], Norbert Ankri[1,2] and Dominique Debanne[1,2]

[1] *INSERM, U641, Marseille, France*
[2] *Université de la Méditerranée, Faculté de Médecine secteur nord, IFR 11, Marseille, France*

Non-technical summary We determined here the role of the hyperpolarization-activated cationic (h) current on the temporal organization of hippocampal activity *in vitro*. In CA1 pyramidal neurons the h-current has three main actions. In addition to setting intrinsic resonance frequency at ∼4 Hz, the h-current determines, through two main mechanisms, the temporal precision of action potentials evoked by excitatory postsynaptic potentials or following stimulation of inhibitory postsynaptic potentials (rebound spiking). We propose that h-channels participate in the fine tuning of oscillatory activity in hippocampal and neocortical networks.

Abstract Hyperpolarization-activated cyclic nucleotide modulated current (I_h) sets resonance frequency within the θ-range (5–12 Hz) in pyramidal neurons. However, its precise contribution to the temporal fidelity of spike generation in response to stimulation of excitatory or inhibitory synapses remains unclear. In conditions where pharmacological blockade of I_h does not affect synaptic transmission, we show that postsynaptic h-channels improve spike time precision in CA1 pyramidal neurons through two main mechanisms. I_h enhances precision of excitatory post-synaptic potential (EPSP)–spike coupling because I_h reduces peak EPSP duration. I_h improves the precision of rebound spiking following inhibitory postsynaptic potentials (IPSPs) in CA1 pyramidal neurons and sets pacemaker activity in stratum oriens interneurons because I_h accelerates the decay of both IPSPs and after-hyperpolarizing potentials (AHPs). The contribution of h-channels to intrinsic resonance and EPSP waveform was comparatively much smaller in CA3 pyramidal neurons. Our results indicate that the elementary mechanisms by which postsynaptic h-channels control fidelity of spike timing at the scale of individual neurons may account for the decreased theta-activity observed in hippocampal and neocortical networks when h-channel activity is pharmacologically reduced.

(Resubmitted 18 March 2011; accepted after revision 27 May 2011; first published online 30 May 2011)
Corresponding author D. Debanne: Université de la Méditerranée, Faculté de Médecine secteur nord, IFR 11, Marseille, France. Email: dominique.debanne@univmed.fr

Abbreviations AHP, afterhyperpolarization; AIS, axon initial segment; 4-AP, 4-aminopyridine; CCh, carbachol; FFT, fast-Fourier transform; HCN, hyperpolarization-activated cyclic nucleotide-gated channels; IR, infra-red.

P. Gastrein and É. Campanac contributed equally to this work.

DOI: 10.1113/jphysiol.2011.209148

Introduction

Hyperpolarization-activated cyclic nucleotide-gated (HCN or h) channels are widely expressed in cortical neurons including pyramidal cells (Maccaferri *et al.* 1993; Pape, 1996; Magee, 1998) and GABAergic interneurons (Maccaferri & McBain, 1996; Aponte *et al.* 2006; Rateau & Ropert, 2006). Their biophysical properties and subcellular localization in the dendrites (Magee, 1998; Lorincz *et al.* 2002) and the axon (Aponte *et al.* 2006) make them key players in controlling information processing in the brain. h-Channels sharpen EPSPs (Magee, 1998) and IPSPs (van Brederode & Spain, 1995) as a result of I_h deactivation and activation, respectively. In addition, these channels are also activated during the medium afterhyperpolarization (Storm, 1989; Gu *et al.* 2005).

Although the contribution of h-channels in pacemaker activity has been demonstrated in cardiac and thalamic cells (Bal & McCormick, 1996; Luthi & McCormick, 1998; Robinson & Siegelbaum, 2003), their precise role in determining the temporal organization of network activity remains poorly understood in the cortex and hippocampus. Theoretical studies suggest that h-channels may control rhythmic activity in hippocampal networks (Rotstein *et al.* 2005; Orban *et al.* 2006) but the experimental demonstration of the importance of h-channels in hippocampal rhythms remains unclear and controversial. For instance, theta (θ) activity in the hippocampus is dramatically disorganized by pharmacological blockade of h-channels with 100 μM ZD-7288 (Cobb *et al.* 2003), but paradoxically left unaffected in HCN1 knock-out mice (Nolan *et al.* 2004). In the developing hippocampus, giant-depolarizing potentials (GDPs) are disrupted by ZD-7288 (Bender *et al.* 2005). However, h-channel blockers reduce epileptiform activity (Kitayama *et al.* 2002) and leave the frequency of neocortical oscillations produced by partial disinhibition unchanged (Castro-Alamancos *et al.* 2007). The role of h-channels in the resonance of the membrane potential at θ-like frequency (range 3–12 Hz) has been demonstrated in CA1 (Hu *et al.* 2002), L5 (Ulrich, 2002) pyramidal cells and in stellate cells of the entorhinal cortex (Dickson *et al.* 2000; Haas *et al.* 2007). Recently, the depolarizing action of I_h has been shown to promote coincidence detection in CA1 neurons (Pavlov *et al.* 2011). However, it is still unclear whether I_h also sets the resonance in CA3 pyramidal cells and GABAergic interneurons, two neuronal populations that play a critical role in hippocampal network activity (Traub *et al.* 1989; Maccaferri & McBain, 1996; Chapman & Lacaille, 1999; Pike *et al.* 2000; Lawrence, 2008; Griguoli *et al.* 2010). Finally, the precise role of I_h in the functional coupling between excitatory or inhibitory synaptic potentials and action potentials remains obscure.

We report here using adequate pharmacological tools and the dynamic-clamp technique that I_h determines the temporal precision of the action potential generated by EPSPs (EPSP–spike coupling) or IPSPs (rebound spiking). EPSP–spike coupling is temporally precise because I_h reduces EPSP duration whereas IPSP–spike coupling is reliable because h-channels accelerate the rate of membrane repolarization after each IPSP. Together with the previously identified actions of I_h on intrinsic resonance and pacemaker activity, these two mechanisms may promote and improve the regularity of network activity in the θ frequency range.

Methods

Slice preparation and electrophysiology

Cortical and hippocampal slices (350–400 μm) were obtained from 10- to 20-day-old rats. All experiments were carried out according to the European and Institutional guidelines for the care and use of laboratory animals (Council Directive 86/609/EEC and French National Research Council). In addition, our experiments comply with *The Journal of Physiology*'s policy on animal experimentation (Drummond, 2009). Briefly, rats were deeply anaesthetized with chloral hydrate (intraperitoneal, 200 mg kg^{-1}) and killed by decapitation. Slices were cut in a solution containing (in mM): sucrose, 280; $NaHCO_3$, 26; D-glucose, 10; KCl, 1.3; $CaCl_2$, 1; $MgCl_2$, 10; and were bubbled with 95% O_2–5% CO_2, pH 7.4. The slices were maintained for 1 h at room temperature in oxygenated (95% O_2–5% CO_2) artificial cerebrospinal fluid (ACSF; in mM: NaCl, 125; KCl, 2.5; NaH_2PO_4, 0.8; $NaHCO_3$, 26; $CaCl_2$, 3; $MgCl_2$, 2; D-glucose, 10). The calcium concentration used here (3 mM) was slightly higher than the physiological level to obtain robust unitary and multi-unitary synaptic potentials. The properties of I_h are thought to be unchanged given the negligible permeability of h-channels to calcium ions (Biel *et al.* 2009). Each slice was transferred to a temperature-controlled recording chamber with oxygenated ACSF. Neurons were visualized in DIC infrared (IR)-videomicroscopy for patch experiments. For whole-cell recordings from cortical L5 and CA1 pyramidal neuron, the electrodes were filled with an internal solution containing (in mM): potassium gluconate, 120; KCl, 20; Hepes, 10; EGTA, 0.5; $MgCl_2$, 2; Na_2ATP, 2.

EPSP–spike coupling was investigated in CA1 pyramidal cells in the presence of the $GABA_A$ receptor blocker picrotoxin (PiTX, 100 μM). In these conditions, the CA3 area was surgically isolated from the CA1 area in order to avoid spontaneous burst discharge. IPSP–spike coupling was investigated in the presence of kynurenate (2 mM, but no PiTX) to evoke monosynaptic IPSPs with electrical stimulation in the cell-body layer. To record

hyperpolarizing $GABA_A$ receptor mediated PSPs (i.e. reversal potential for chloride $= -70$ mV) the intra-pipette chloride concentration was reduced to 8.6 mM (mM: potassium gluconate, 150; Hepes, 10; EGTA, 0.5; KCl, 4.6; $MgCl_2$, 2; Na_2ATP, 2; NaGTP, 0.3; phosphocreatine, 10).

Pairs of CA3 pyramidal neurons were recorded in organotypic slice cultures (Boudkkazi *et al.* 2007; Debanne *et al.* 2008; Boudkkazi *et al.* 2011), in order to identify excitatory monosynaptic connections and test the specificity of the h-channel blocker ZD-7288. Hippocampal slice cultures were prepared as described previously (Stoppini *et al.* 1991; Debanne *et al.* 2008). Briefly, postnatal day 5–7 Wistar rats were deeply anaesthetized by intraperitioneal injection of chloral hydrate, the brain was removed and each hippocampus was individually dissected. Hippocampal slices (300 μm) were placed on 20 mm latex membranes (Millicell) inserted into 35 mm Petri dishes containing 1 ml of culture medium and maintained for up to 21 days in an incubator at 34°C, 95% O_2–5% CO_2. The culture medium contained (in ml) 25 minimum essential medium (MEM), 12.5 Hank's balanced salt solution (HBSS), 12.5 horse serum, 0.5 penicillin/streptomycin, 0.8 glucose (1 M), 0.1 ascorbic acid (1 mg ml^{-1}), 0.4 Hepes (1 M), 0.5 B27, 8.95 sterile H_2O. To limit glial proliferation, 5 μM Ara-C was added to the culture medium starting at 3 DIV.

In a few experiments, field-potentials were recorded in the cell body layer (stratum pyramidale of the CA1 region or in L5 of the neocortex) using glass microelectrodes filled with 3 M NaCl. Glass stimulating electrodes filled with extracellular saline were placed in the stratum radiatum.

Drugs were bath applied. PiTX, kynurenate and bicuculline methiodide were purchased from Sigma-Aldrich and ZD-7288 from Tocris-Cookson. All recordings were made at 29°C (except for experiments in neocortical slices, 32°C).

Data acquisition and analysis

Electrophysiological recordings were obtained using an Axoclamp-2B or an Axopatch-200B amplifier (Axon Instruments, Union City, CA, USA), Acquis1 software (Bio-Logic, Orsay, France) or pCLAMP v. 8 or 9 (Axon Instruments). Data were analysed with Igor Pro v. 5 or v. 6 (WaveMetrics, Lake Oswego, OR, USA) or home-made software (PERL, written in Linux). Pooled data are presented as means ± SEM and statistical analysis was performed using the Mann–Whitney *U* test, Wilcoxon's test or Student's paired *t* test.

Auto- and cross-correlation functions were calculated from the membrane potential recordings with a PERL programmed script and then normalized. To quantify the coherence and amplitude of the oscillation, we used the method described in Bringuier *et al.* (1997). Briefly, voltage recordings were filtered to remove signals faster than 10 mV ms^{-1}. The autocorrelation function was computed and optima in the autocorrelogram were detected with a PERL routine (red dots in Supplementary Fig. 1*A*). An evaluation of the period of oscillation is given by the intervals between maxima and minima (I_1 to I_6, Supplementary Fig. 1*A*). The coefficient of oscillation (C_o) was determined as the ratio of the standard deviation (SD) over the mean to quantify the temporal coherence of the oscillation. Lower C_o indicates higher temporal coherence. The amplitude of oscillation (A_o) was determined by the amplitude between the first minimum and the average of the first two maxima (Supplementary Fig. 1*B*). This method was preferred to the power spectrum analysis because it specifically evaluates the coherence of oscillations.

Simulated synaptic waveforms were generated with a double exponential function, $f(t) = a(1 - \exp(-t/\tau_{ON}))\exp(-t/\tau_{OFF})$, with $\tau_{ON} = 0.5$ ms, $\tau_{OFF} = 10$ ms.

Recording and analysis of electrical resonance

The impedance amplitude profile (ZAP) method was used to characterize the electrical resonance of interneurons (Hutcheon & Yarom, 2000; Hu *et al.* 2002). Briefly, a sinusoidal current with constant amplitude and linearly increasing frequency (0–10 Hz for 30 s) was injected in the recorded electrode and the voltage response was recorded. Resonance was signalled by a distinct peak in the voltage response. The cell impedance as a function of frequency was given by the ratio of the fast-Fourier transform (FFT) of the voltage response to the magnitude of the FFT of the input current. The strength of the resonance was quantified by the *Q* value, i.e. the ratio of the impedance at the resonance peak to the impedance at 0.5 Hz (Hutcheon *et al.* 1996; Hu *et al.* 2002).

Model of the h-conductance (G_h)

Biophysical characterization of I_h was assessed in CA1 pyramial neurons in the presence of TTX (500 nM), PiTX (100 μM), kynurenate (2 mM), Ni^{2+} (200 μM), TEA (5 mM) and 4-AP (100 μM). To block h-channels in the absence of synaptic transmission, a high concentration of ZD-7288 (50–100 μM) was applied (Campanac *et al.* 2008). Subtraction of control records from those obtained after ZD-7288 application allowed isolation of h-currents. Activation was assessed by voltage steps from a holding potential of −50 mV to −60/−120 mV. Deactivation was analysed in tail currents evoked by stepping from −75 mV to −70/−45 mV. All current traces evoked were fitted with mono-exponential functions. Reversal potential (E_h)

was determined by linear extrapolation of the tail-current amplitude. E_h was -37.7 ± 0.9 mV ($n = 3$).

Equations describing the voltage dependence of G_h were based on a deterministic Hodgkin–Huxley model with one variable (n, the gating particle for activation) which obeys first order kinetics. The h-current was given by: $I_h = G_h(V_m - E_h)$, with V_m the membrane potential, $E_h = -37.7$ mV, and the h-conductance $G_h = G_{h,max}n$. The activation and deactivation time constants were determined by fitting experimental data (see above).

The differential equation $dn(V,t)/dt = \alpha(V)[1 - n(V,t)] - \beta(V)n(V,t)$ was solved. This equation corresponds to $d(V,t)/dt = [n_\infty(V) - n(V,t)]/\tau(V)$ with the steady-state activation parameter as $n_\infty(V) = \alpha_n(V)/[\alpha_n(V) + \beta_n(V)]$, and the activation time constant $\tau(V) = 1$ for $V > -30$ mV otherwise $\tau(V) = 1/[\alpha_n(V) + \beta_n(V)]$ with:

$$\alpha_n = 0.0204/1 + \exp[(V + 98.68)/13.24]$$

$$\beta_n = 0.0176/1 + \exp[-(V + 57.96)/13.2]$$

Dynamic clamp

To add an artificial I_h conductance in CA1 pyramidal neurons, a fast dynamic-clamp system was developed (Sharp *et al.* 1993; Prinz *et al.* 2004; Carlier *et al.* 2006; Campanac *et al.* 2008). The system consisted of an embedded processor with real-time operating system which was programmed and controlled from a host PC with the graphical language LabView 7-Express containing the LabView Real-Time module. The feedback loop ($F = 38$ kHz) continuously read the membrane potential V_m from the Axoclamp-2B, computed G_h and generated an output, I_h, according to the equation: $I_h = G_h(V_m - E_h)$. A reconfigurable I/O module (NI PXI-7831R) allowed monitoring of V_m and generation of I_h. The access speed of analog–digital and digital–analog conversions on the input/output module was optimized by a field-programmable gate array.

To minimize calculations during the calculation loop, specific arrays of $\tau(V)$ and $n_\infty(V)$ were initialized with a resolution of 0.1 mV. For a given voltage, corresponding values of $\tau(V)$ and $n_\infty(V)$ were obtained by linear interpolation from the array. The numerical integration, based on Euler's method, involved a simple linear extrapolation of the gating variable given by the equation: $n_{k+1} = n_k + (n_\infty - n_k)dt$

An Axoclamp 2B amplifier (Axon Instruments) was used for dynamic-clamp experiments and the bridge balance was monitored continuously to minimize series resistance artifacts. Only recordings with series resistance <25 MΩ were kept for further analysis.

The models were validated with addition and subtraction of the h-conductance (Campanac *et al.* 2008). Families of voltage traces evoked by depolarizing and hyperpolarizing pulses of current (+50/−50 pA) were recorded in controls. In the presence of 5 mM Cs^+ in the external saline the input resistance increased and the depolarizing sag was suppressed. The addition of the simulated h-conductance with the dynamic clamp (range: 5–7 nS, $n = 3$) decreased the input resistance and restored the sag (see Campanac *et al.* 2008). In fact, voltage signals recorded in these conditions were virtually identical to the control traces. An external digital device (Microchip Technology Inc., Chandler, Arizona, USA) was used to facilitate the adjustment of the values of G_h during the experiment. Thus, digitized values of this variable were directly read in real time by the I/O module.

Results

Pharmacological blockade of h-channels without affecting synaptic transmission

Studying the role of h-current on the timing of synaptically evoked action potentials implies to preliminarily determine the specificity of the pharmacological blockers of I_h. ZD-7288 is a potent inhibitor of I_h but it also reduces presynaptic transmitter release (Chevaleyre & Castillo, 2002). h-Channels are localized in hippocampal axons (Soleng *et al.* 2003) and synaptic transmission might be reduced because ZD-7288-induced hyperpolarization of axons either reduces axonal excitability or presynaptic release (Saviane *et al.* 2003; Shu *et al.* 2006). We have therefore re-examined the effects of ZD-7288 at excitatory synapses formed by connected CA3 pyramidal neurons in organotypic slice cultures in which the generation of the presynaptic spike and the presynaptic voltage are controlled. In these experiments, presynaptic voltage was maintained constant. At 1 μM, ZD-7288 clearly blocked I_h because the amplitude of the depolarizing sag was abolished and the apparent input resistance increased ($143 \pm 8\%$ of the control, $n = 6$, Fig. 1*A*). However, no reduction in synaptic strength was observed at CA3–CA3 unitary synapses ($97 \pm 13\%$ of the control EPSP amplitude $n = 6$, Wilcoxon's test, $P > 0.2$; Fig. 1*A*). Application of ZD-7288 at 100 μM fully blocked transmission ($7 \pm 10\%$ of the control EPSP amplitude, $n = 4$, Wilcoxon's test, $P < 0.01$; Fig. 1*B*). Synaptic transmission was also reduced by 20 μM ZD-7288 ($77 \pm 15\%$ of the control EPSP amplitude, $n = 4$; Fig. 1*C*). To confirm these results obtained in slice cultures, additional experiments were performed in CA1 pyramidal neurons from acute slices. Bath application of 1 μM ZD-7288 did not reduce excitatory synaptic transmission ($110 \pm 2\%$, of the control EPSP slope measured 10 min after application $n = 6$; Supplementary Fig. 2). In conclusion, our data indicate

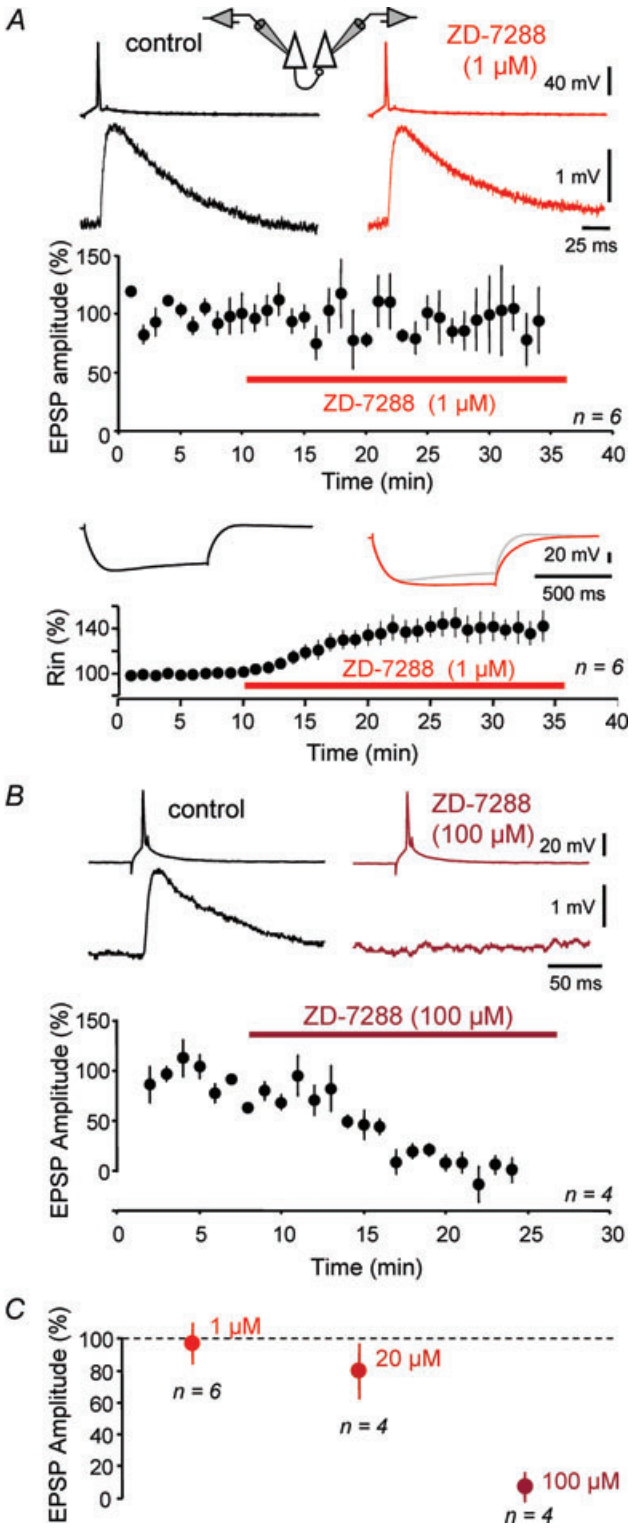

Figure 1. Pharmacological specificity of the h-channel blocker ZD-7288 at synapses formed by connected pairs of CA3 pyramidal neurons in organotypic slice cultures
A, postsynaptic h-current but not synaptic transmission is blocked with 1 μM ZD-7288. Top, representative traces of presynaptic spikes, EPSPs and voltage deflections in response to hyperpolarizing current steps (150 pA), before (control) and 20 min after bath application of ZD-7288 (1 μM). Bottom, time course of the normalized EPSP amplitude. Note the stability of synaptic transmission. *B*, block of synaptic transmission with 100 μM ZD-7288. Note the large reduction in EPSP amplitude 15 min after application of 100 μM ZD-7288 (top traces and time course of EPSP amplitude). *C*, summary of the changes in EPSP amplitude induced by ZD-7288 measured at 15–20 min.

that ZD-7288 must be applied at 1 μM to block postsynaptic h-channels without affecting excitatory synaptic transmission.

We next determined whether the h-current was blocked comparably by 1 μM ZD-7288 or 2.5 mM external Cs^+. CA1 pyramidal neurons were recorded in voltage-clamp (holding potential, $V_h = -60$ mV). An inward current was evoked by a hyperpolarizing pulse to -90 mV. In these experiments, the capacitive and leak currents were not subtracted. Consecutive bath application of Cs^+ (2.5 mM) and ZD-7288 (1 μM) blocked the slow current similarly (Cs^+-sensitive component $= 108 \pm 10$ pA and ZD-sensitive component $= -100 \pm 8$ p-108, $n = 5$, Wilcoxon's test, $P > 0.1$; Fig. 2). We conclude that the postsynaptic h-current is blocked to the same extent by 2.5 mM external Cs^+ or 1 μM ZD-7288.

h-Channels determine the temporal precision of EPSP-spike coupling

Transmission of temporally organized input patterns represents a critical operation achieved by cortical networks. For instance, subthreshold excitatory potentials occasionally evoke APs in CA1 pyramidal neurons during induction of *in vitro* oscillation activity in the hippocampal network with bath application of carbachol (CCh, 50 μM, Fig. 3*A*). The coherence of network activity will be preserved in the circuit if principal neurons reliably transmit temporal input patterns downstream. We therefore tested the effects of h-channel blockers on EPSP-spike coupling in CA1 pyramidal neurons. In these experiments, the stimulus intensity was adjusted to produce a spike in about half of the trials and the shift in membrane potential induced by the h-channel blocker was compensated with constant holding current. Thus, the precision was estimated before and after blockade of h-channels in similar conditions. In the presence of external Cs^+ (2.5 mM; Fig. 3*B*) or ZD-7288 (1 μM; Fig. 3*C*), the latency of the AP evoked by the EPSP was found to be more variable from trial to trial compared to controls (SD in controls: 5.3 ± 0.5 ms; SD in the presence of h-channel blocker: 18.0 ± 3.9 ms, $n = 15$, Wilcoxon's test, $P < 0.01$, Fig. 3*D*). The EPSP–spike precision was reduced because the duration of subthreshold EPSPs at nearly maximal depolarized potential was enhanced in the presence of h-channel blockers. In fact, the duration of the EPSP at 90% of its amplitude was significantly longer in the

presence of h-channel blocker (in controls: 24 ± 1 ms, in the presence of h-channel blockers: 48 ± 4 ms, $n = 15$; Fig. 3*E*). Interestingly, the normalized EPSP duration at 90% and the normalized SD were positively correlated ($R^2 = 0.84$, Fig. 3*F*), indicating that EPSP–spike precision depends tightly on the duration of the EPSP at the peak.

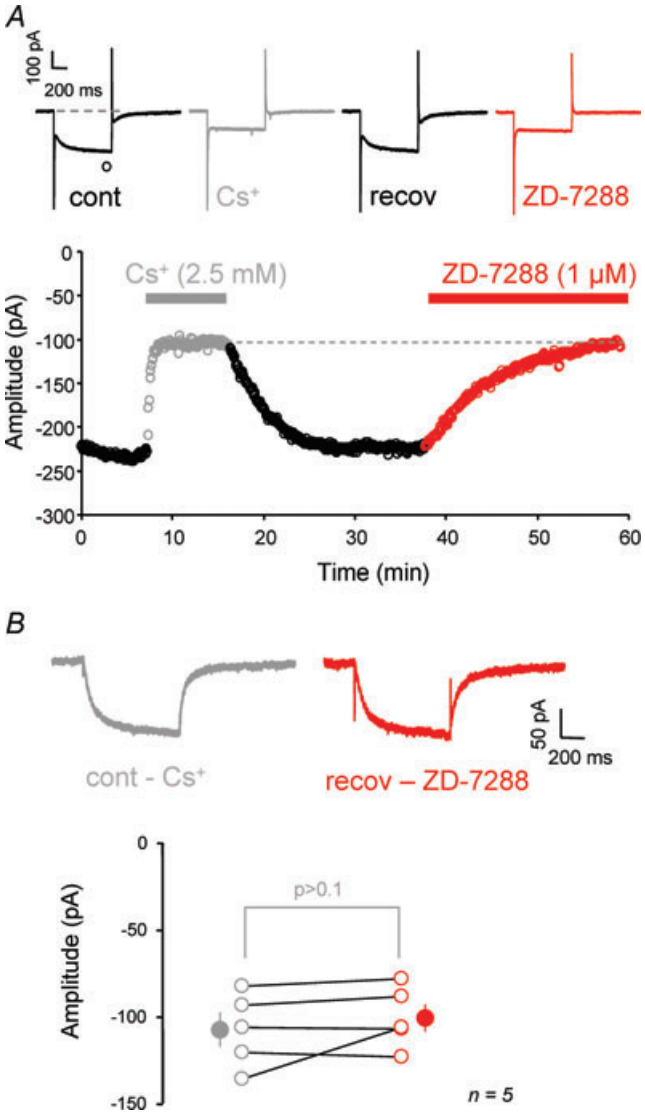

Figure 2. Comparison of the effects of external Cs^+ and ZD-7288 on h-currents recorded from CA1 pyramidal neurons in acute slices
A, top, representative current traces evoked by hyperpolarizing pulses from −60 to −90 mV in control (black), after successive applications of 2.5 mM Cs^+ and 1 μM ZD-7288. Bottom, time course of the current amplitude measured from the baseline to the end of the pulse (symbol on the top left trace). Note the blockade of the slowly activating inward current with Cs^+ or ZD and its full recovery to the control level after washing Cs^+ out. *B*, comparison of the currents blocked by Cs^+ and ZD in 5 experiments. Top, representative traces of the Cs^+- and the ZD-sensitive currents in the cell illustrated in *A*. Bottom, graph of the Cs^+- and ZD-sensitive currents recorded in 5 neurons.

We next determined whether enhancement of I_h improved EPSP–spike precision. Since pharmacological activators of h-channels such as lamotrigine (Poolos *et al.* 2002) are not highly selective for these channels but also block Na^+ and A-type K^+ currents (Remy *et al.* 2003; Huang *et al.* 2004), we used the dynamic-clamp technique to add h-conductance (G_h). The addition of G_h (10 nS) reduced the apparent input resistance and increased the amplitude of the depolarizing sag (Fig. 4*A*). In these conditions the spike jitter was reduced (SD = 3.4 ± 0.4 ms in control and SD = 2.4 ± 0.5 ms ($n = 5$) when G_h was added, Wilcoxon's test, $P < 0.05$; Figs 4*B* and 3*C*) and the duration of the EPSP at 90% of its amplitude was reduced (15.9 ± 1.2 ms *vs.* 14.0 ± 1.1 ms, $n = 5$; Wilcoxon's test, $P < 0.05$, Fig. 4*D*). Thus, h-channels improve temporal precision of EPSP–spike coupling by reducing the temporal window during which an AP might be elicited.

We next analysed how I_h was activated during an EPSP. CA1 pyramidal neurons were voltage clamped and the currents generated by an EPSP waveform (holding potential −70 mV, amplitude 17–30 mV, sum of two exponentials with a rise time of 10 ms and a decay time constant of 50 ms) were recorded (Fig. 5*A*). The current sensitive to ZD-7288 was outward and temporally coincided with the decay of the EPSP (Fig. 5*B*). The rise time of the ZD-7288-sensitive current evoked by a 30 mV EPSP waveform was 38 ± 4 ms ($n = 3$). Thus, the depolarization elicited by an EPSP deactivates h-channels and is equivalent to a fictive outward current that accelerates the rate of repolarization after the peak of the EPSP and reduces the time window during which an AP can be generated. Our data further support the rule governing EPSP–spike precision where outward currents coinciding with the decay of the EPSP improve spike time precision (Fricker & Miles, 2000; Pouille & Scanziani, 2001; Axmacher & Miles, 2004).

In conclusion, h-channels improve the temporal precision of the EPSP–spike coupling because h-channels accelerate the decay of EPSPs and thus reduce the time during which an AP can be triggered by the EPSP.

h-Channels enhance the precision of IPSP–spike coupling in CA1 pyramidal neurons

Basket cells synchronize pyramidal cell firing through rebound excitation produced by IPSPs (Cobb *et al.* 1995; Klausberger & Somogyi, 2008). In fact, during bath application of CCh, hippocampal neurons were depolarized near to their spike threshold and fast hyperpolarizing postsynaptic potentials at a frequency of ~6 Hz were occasionally observed, which triggered rebound action potentials (Fig. 6*A*). Synchronization between neurons receiving a common inhibitory input might

be improved by I_h because it accelerates the rate of membrane depolarization during the IPSP. We therefore examined whether the precision of IPSP-spike coupling was affected by h-channel blockers. CA1 pyramidal neurons were whole-cell recorded with a pipette solution containing a low concentration of chloride ions (see Methods) and monosynaptic IPSPs were evoked in the presence of 2 mM kynurenate with a stimulating electrode

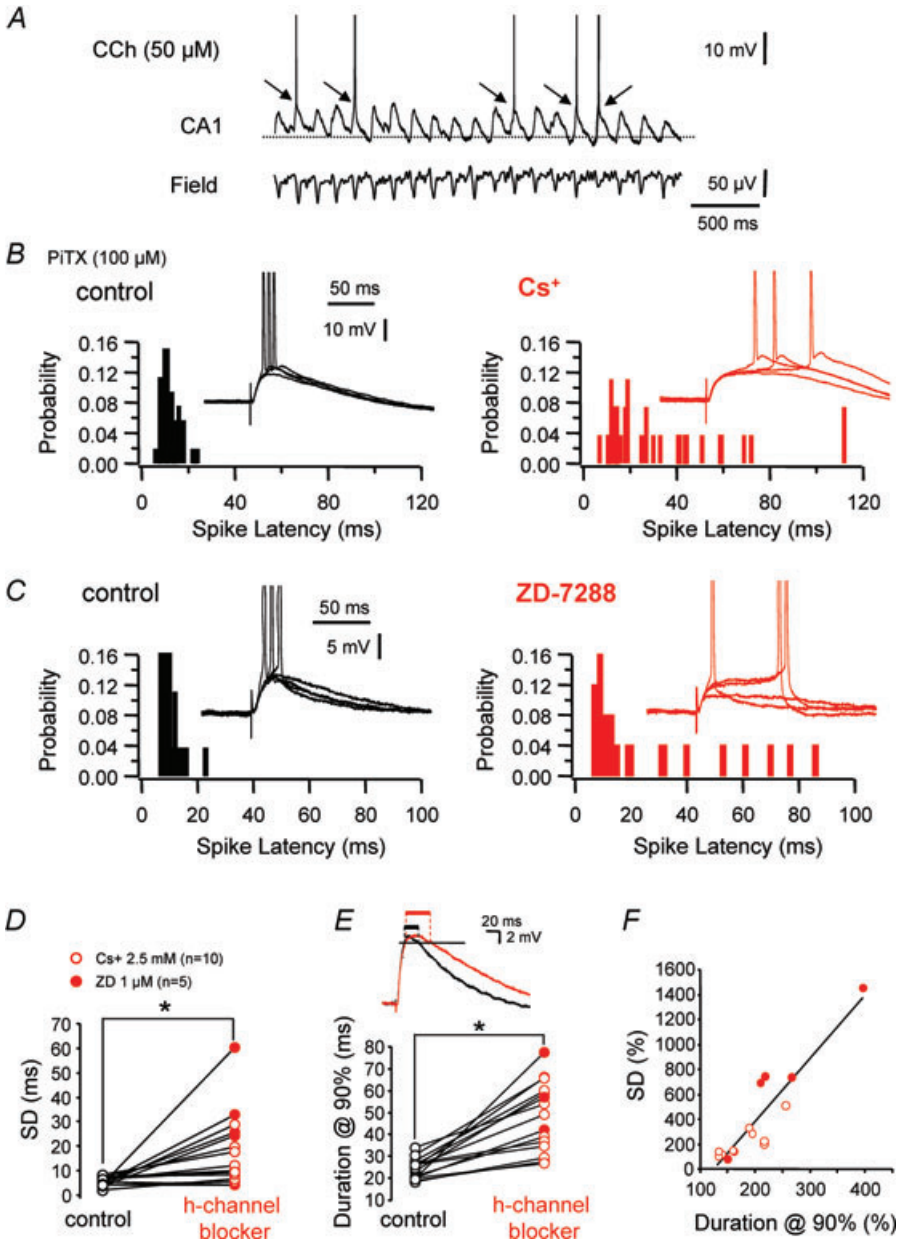

Figure 3. h-Channels determine the precision of EPSP-spike coupling in CA1 pyramidal neurons in acute hippocampal slices

A, EPSP–spike coupling during theta-oscillations. *B* and *C*, effects of external Cs^+ (*B*) and ZD-7288 (*C*) on the precision of EPSP–spike coupling. In all cases, EPSPs were evoked in the presence of 100 μM PiTX by the stimulation of the Schaffer collaterals to produce in nearly 50% of the trials a postsynaptic AP. Left, control condition. Top, representative traces. Bottom, histogram of postsynaptic APs. Right, EPSP–spike coupling in the presence of 2.5 mM Cs^+ (*B*) or 1 μM ZD-7288 (*C*). *D*, analysis of the standard deviation (SD) of AP latency in controls and in the presence of h-channel blockers (*$P < 0.01$, Wilcoxon's test). *E*, effect of h-channel blockers on the duration of the maximal depolarization of EPSP (90%). Top, representative traces in controls (black) and in the presence of h-channel blockers (red). Bottom, summary of the quantification of the EPSP duration measured at 90% of its maximal amplitude (*$P < 0.05$, Wilcoxon's test). *F*, normalized SD as a function of normalized EPSP duration at 90% induced by h-channel blockers. Black line, linear regression ($y = 5.07x - 632$, $R^2 = 0.84$).

located in the pyramidal cell layer to preferentially activate basket cells. The pyramidal neuron was held near −50 mV by injection of constant depolarizing current (range +10/+30 pA) to produce spontaneous spike firing. Rebound spikes were evoked by the IPSP in a narrow time window (Fig. 6*B*). Bath application of external caesium (2.5 mM) disorganized rebound spiking. Fitting histograms of the first spikes with Gaussians revealed that the dispersion was significantly higher in the presence of external Cs^+ (in controls, SD = 137 ± 17 ms; in the presence of h-channel blockers, SD = 173 ± 15 ms, $n = 12$; paired t test, $P < 0.02$). The loss of temporal precision could be attributed to a change in the rate of membrane depolarization before spike generation (Sourdet *et al.* 2003; Cudmore *et al.* 2010). In fact, the IPSP decay slope was found to be reduced in the presence of Cs^+ (29.9 ± 4.3 mV s^{-1} in controls *vs.* 22.7 ± 4.0 mV s^{-1} in the presence of h-channel blocker, $n = 12$; paired t test, $P < 0.01$; Fig. 6*C*). Thus, our results indicate that the shaping of the IPSP by h-channels allows temporally precise rebound firing through an acceleration of the rate of membrane depolarization before spike generation.

h-Channels control the resonance frequency in CA1 oriens interneurons

h-Channels set the resonance frequency in hippocampal (Hu *et al.* 2002) and cortical pyramidal neurons (Ulrich,

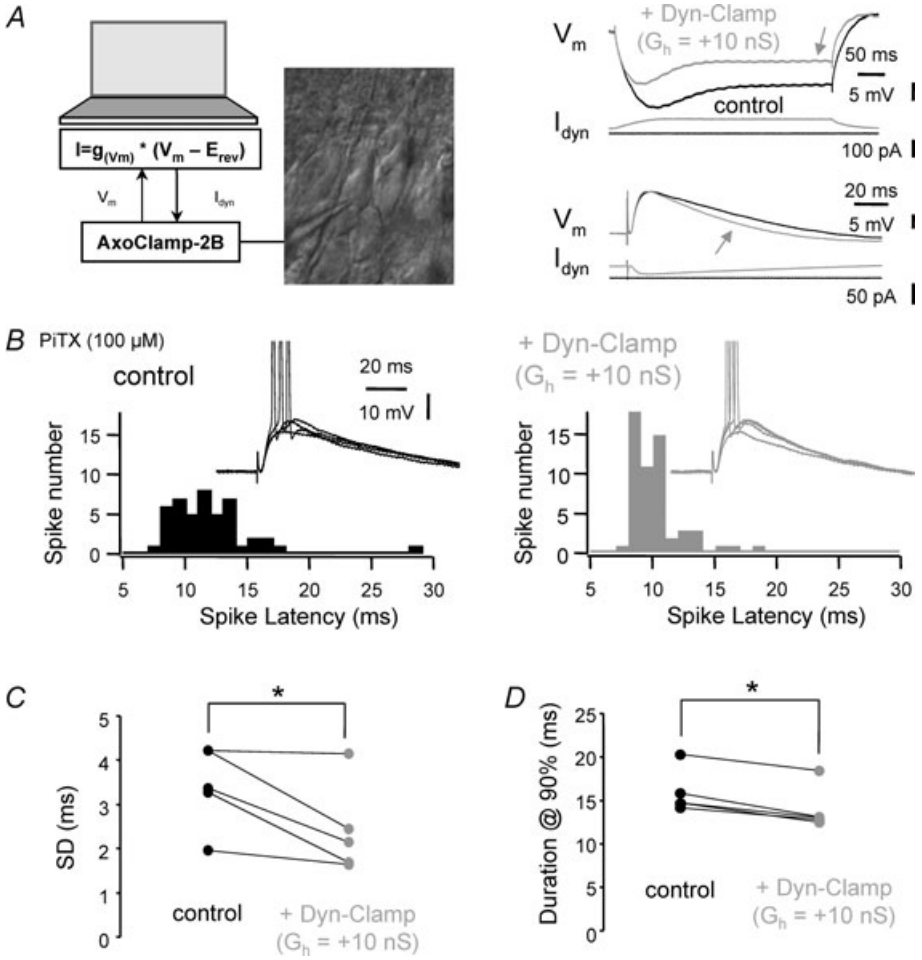

Figure 4. Addition of exogenous h-conductance (G_h) with dynamic current-clamp improves EPSP–spike precision in CA1 pyramidal neurons from acute slices
A, experimental design (left) and effects of addition of G_h on input resistance (top right) and EPSP waveform (bottom right). Note the decrease in the amplitude of hyperpolarization evoked by a pulse of constant current (downward arrow) and the acceleration of the EPSP decay (upward arrow). *B*, improvement of EPSP–spike coupling precision by addition of G_h. Representative voltage traces and histograms of postsynaptic spikes in control conditions (left) and when G_h (+10 nS) was added (right). Here, again, the probability of firing was maintained close to 0.5 in both conditions. EPSP–spike coupling was more precise when G_h was injected. *C*, summary of the effects of G_h on the SD of the postsynaptic spike (*$P < 0.05$, Wilcoxon's test). *D*, effect of G_h addition on the EPSP duration at 90% of its amplitude (*$P < 0.05$, Wilcoxon's test).

2002), but it is not clear whether they control intrinsic membrane resonance in inhibitory interneurons (Pike *et al.* 2000; Storm & Hu, 2003). h-Current is particularly prominent in interneurons from the stratum oriens (Maccaferri & McBain, 1996; Lupica *et al.* 2001). A subpopulation of these cells is sensitive to muscarinic receptor stimulation (Lawrence *et al.* 2006). We therefore examined whether h-channel activity determines the resonance frequency of the membrane potential in these interneurons. Eight interneurons with a horizontal fusiform cell body were recorded in the stratum oriens (Fig. 7*A*). Consistent with the behaviour of oriens interneurons (Maccaferri & McBain, 1996), their action potentials were fast and displayed a prominent AHP. In addition, injection of hyperpolarizing pulses of current evoked large depolarizing sag (arrow Fig. 7*A*). We first studied the impact of the membrane potential on the resonance behaviour of interneurons. The membrane potential was clamped manually at a potential ranging from −55 to −75 mV with the injection of a constant current. A sinusoidal current with constant amplitude but linearly increasing frequency ('chirp') was injected through the recording electrode (0–10 Hz during 30 s; Fig. 7*B*). The resonance frequency was higher for hyperpolarized membrane potential (2.6 ± 0.2 Hz at −75 mV *vs.* 1.5 ± 0.3 Hz at −55 mV, $n = 8$; Fig. 7*B*). In contrast with the U-shaped voltage-dependent resonance reported in CA1 pyramidal cells (Hu *et al.* 2002), the dependence was linear in oriens interneurons (linear fit, $R^2 = 0.88$). To estimate the strength of the resonance we calculated the *Q* value, which is ratio of the impedance at the resonance peak to the impedance at 0.5 Hz (Hu *et al.* 2002). On average, the *Q* value measured at a potential of −65 mV was found to be close to 1.51 ± 0.24 for stratum oriens interneurons ($n = 8$). Most importantly, the resonance behaviour of stratum oriens interneurons was totally suppressed after pharmacological blockade of h-channels with external Cs^+ (2 mM, Fig. 7*C* and *D*). In the presence of external Cs^+, the impedance profile resembled that of a purely passive membrane (Hutcheon & Yarom, 2000). This behaviour was observed in all the interneurons tested ($n = 8$). Thus, h-channels set the resonance frequency near 2–3 Hz in stratum oriens interneurons.

Pacemaker activity in GABAergic interneuron is controlled by h-channels

In the cortex, activity of pyramidal neurons is synchronized by inhibitory interneurons (Cobb *et al.* 1995). GABAergic interneurons from the stratum oriens inhibit the dendrite of CA1 pyramidal neurons. They are depolarized by cholinergic receptors and spontaneously fire at a frequency in the θ range. Although I_h contributes to stratum oriens interneuron pacemaking activity by shaping AHPs (Maccaferri & McBain, 1996), the role of h-channels in determining the temporal regularity of firing remains unclear. We re-examined this question in stratum oriens interneurons from the CA1 region. Interneurons were recorded in the presence of kynurenate and picrotoxin to block fast synaptic transmission. Upon injection of constant depolarizing current (range: +24/+68 pA, maintained constant throughout the experiment), these neurons fired regularly (CV = 0.12 ± 0.02, $n = 11$) at a frequency within the θ-range (5.6 ± 1.9 Hz, $n = 11$; Fig. 8*A*). In the

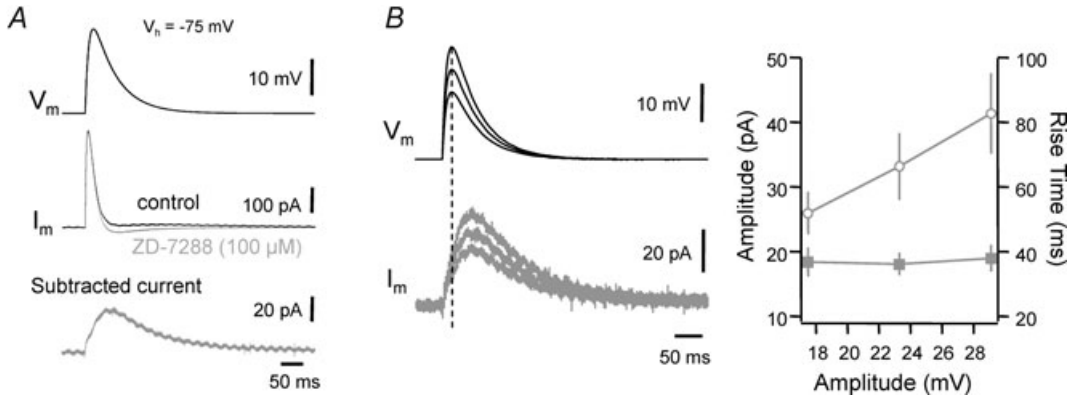

Figure 5. h-Current activated by a somatically injected EPSP waveform in CA1 pyramidal neurons from acute slices
A, voltage-clamp responses to somatic injection of a simulated EPSP waveform. Records were obtained in the presence of blockers of synaptic transmission (2 mM kynurate and 100 μM PiTX) and voltage-gated channels (500 nM TTX, 100 μM 4-AP, 5 mM TEA and 200 μM Ni^+). I_h was isolated by subtracting evoked current in the presence of 50 μM ZD-7288. *B*, time course of h-current activated by an EPSP waveform. Whatever the amplitude of the EPSP waveform used here, the h-current peaked during the falling phase of the EPSP (dashed line, peak of the EPSP waveform). Right, amplitude (circles) and rise time (squares) of ZD-sensitive current *vs.* amplitude of the EPSP waveform.

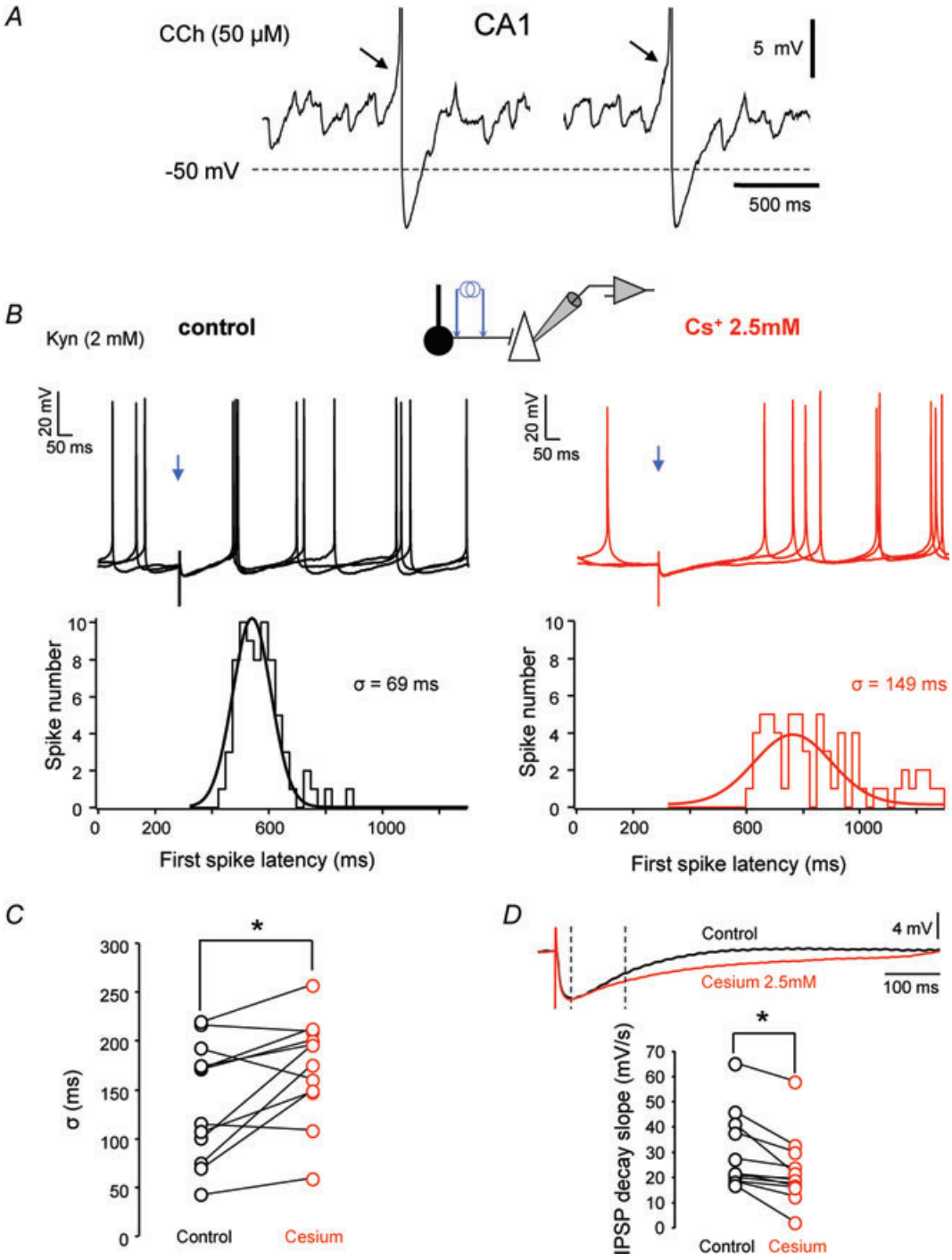

Figure 6. I_h determines the precision of IPSP–spike coupling in CA1 pyramidal neurons from acute slices
A, IPSP–spike sequences observed in a CA1 pyramidal neuron during θ episodes induced by CCh. APs (arrows) are truncated. *B*, IPSP–spike coupling assessed in CA1 pyramidal neurons. The neuron was held near its spike threshold (~−50 mV) by constant current injection. Top, traces from representative trials in control (left) and in the presence of 2.5 mM Cs^+ (right). Bottom, peri-stimulus time histograms of the first spikes. Synaptic stimulation occurred at 200 ms. For practice, histograms of the 1st spikes were fitted with Gaussian functions and in each case the deviation (σ) was determined. *C*, effect of Cs^+ on the deviation (σ) of the rebound spiking activity ($n = 7$ CA1 neurons). *D*, incidence of I_h on the decay of IPSP. Left, subthreshold traces averaged over 25 traces from the experiment illustrated in *B* (black trace, control; red trace Cs^+). Right, plot of the IPSP decay slope in control and in the presence of Cs^+.

presence of external Cs^+/ZD-7288, the mean frequency slightly decreased to 4.3 ± 2.0 Hz ($n = 11$; Wilcoxon's test, $P < 0.01$), as previously observed (Maccaferri & McBain, 1996). Most importantly, the regularity of firing was markedly reduced (CV $= 0.29 \pm 0.05$, $n = 11$, Wilcoxon's test, $P < 0.01$; Fig. 8*A*).

We next determined the origin of this decreased regularity of pacemaker firing. It has been established

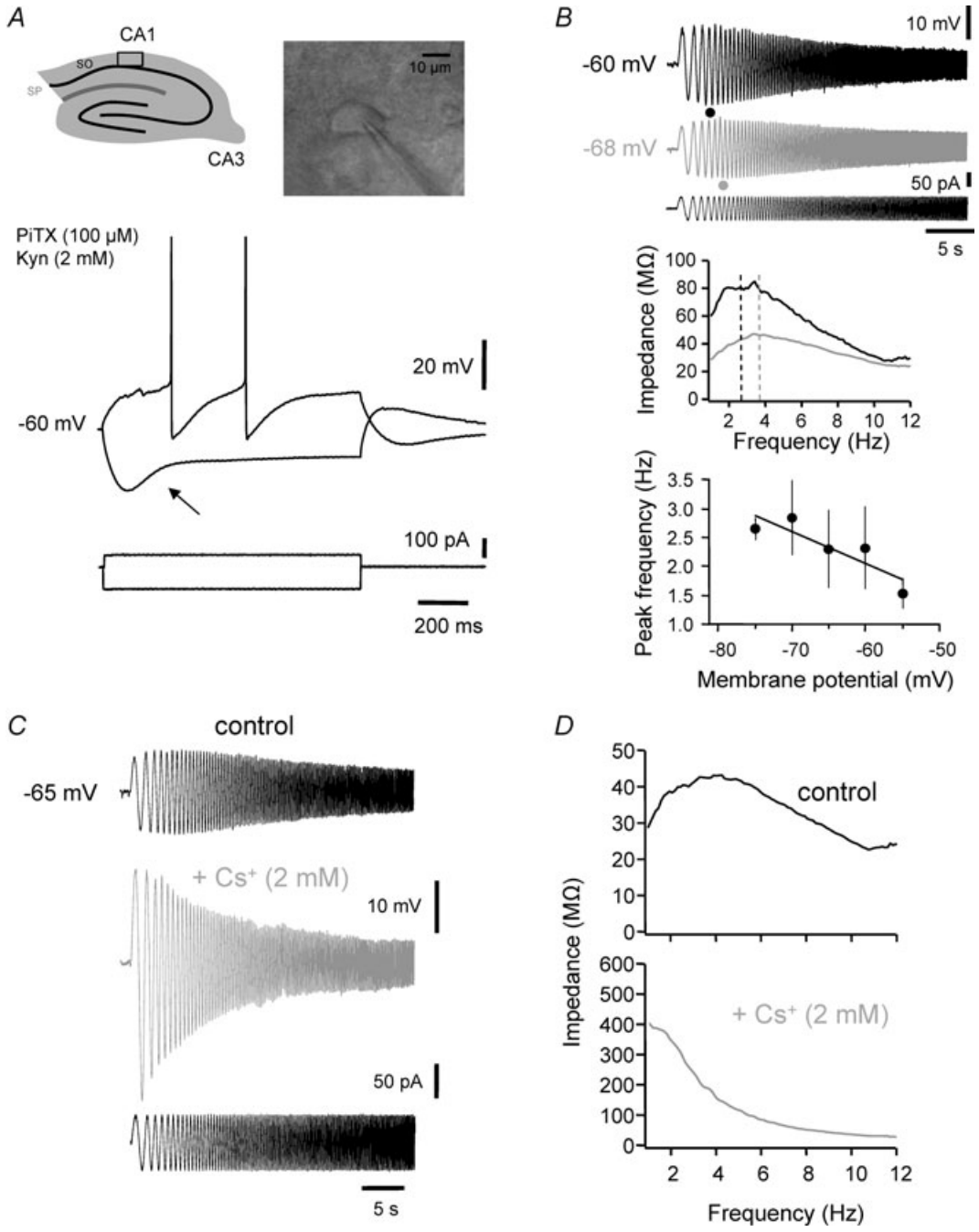

Figure 7. I_h-dependent resonance in stratum oriens interneuron from acute slices
A, physiological characteristics of an oriens interneuron from CA1. Top, DIC-IR picture of the recorded neuron. Bottom, current-clamp response of the neuron. Note the presence of a large depolarizing sag in response to injection of hyperpolarizing current. *B*, voltage dependence of the resonance. Top, representative voltage profiles in response to a sinusoidal current, at two different membrane potentials (−60 mV and −68 mV). Middle, impedance profiles in the two conditions. Note that the peak frequency is higher at −68 mV. Bottom, group data ($n = 8$ cells) showing the peak frequency as a function of membrane potential (linear regression, $y = -0.055x - 1.262$, $R^2 = 0.75$). *C* and *D*, effects of external Cs^+ on the impedance profile of an oriens interneuron.

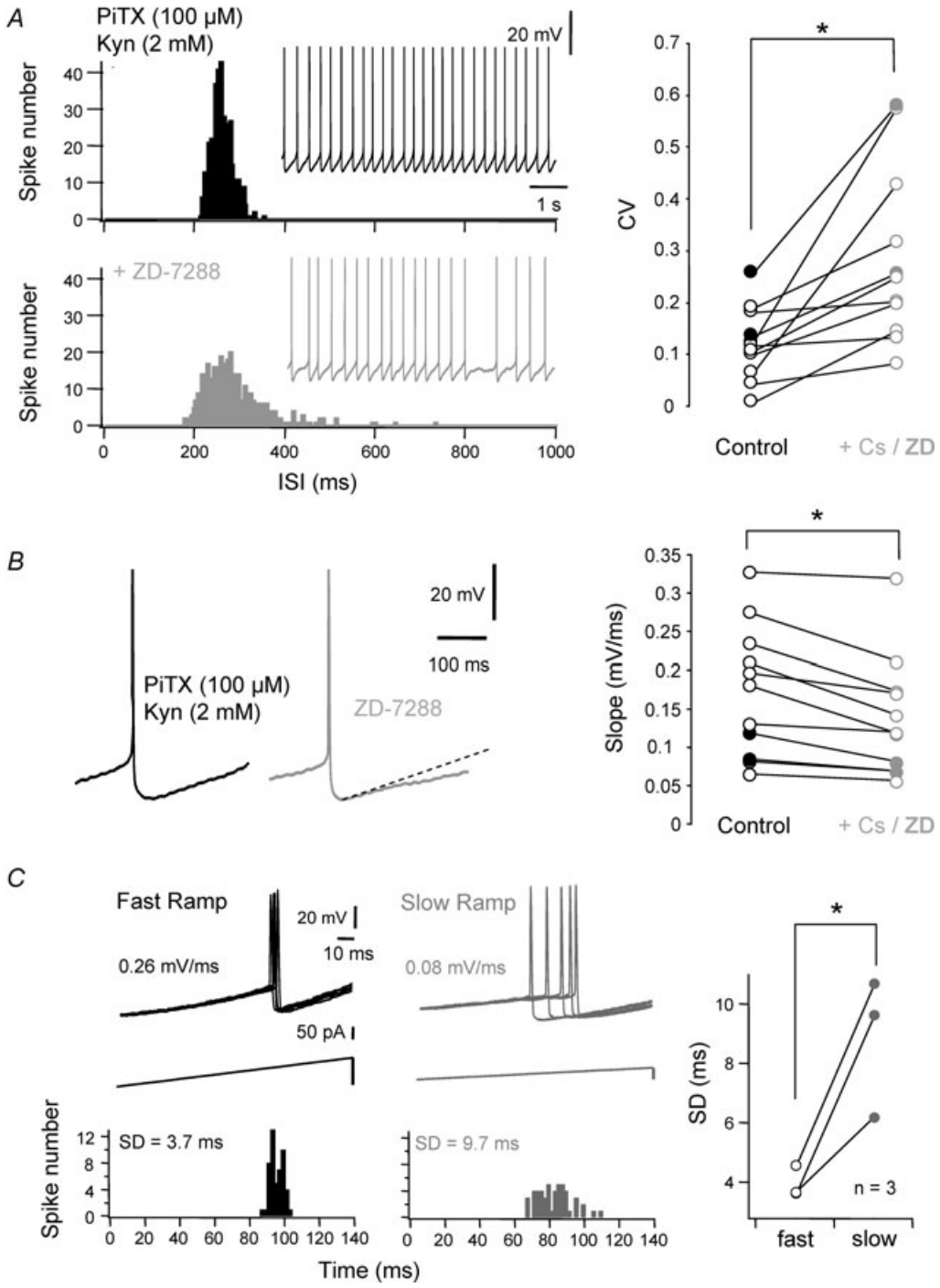

Figure 8. I_h controls pacemaker activity in oriens interneurons
A, effect of external ZD-7288 on pacemaker activity. Top left, control conditions. Bottom left, firing pattern in the presence of 10 μM ZD-7288. Histograms of inter-spike intervals (ISIs) in controls (black histogram) and in the presence of ZD-7288 (grey histogram). Right, coefficient of variation (CV) in controls (○) and in the presence of Cs^+ (○) or ZD (●) analysed in 11 oriens interneurons. *B*, reduced rate of repolarization during the AHP. Left, representative traces in controls (black) and in the presence of ZD (grey). The dashed oblique line indicates the slope of the AHP in control conditions. Right, voltage slope measured during the AHP decay in controls (●) and in the presence of Cs^+ (○) or ZD (●) in 11 oriens interneurons. *C*, the rate of membrane depolarization determines spike precision in oriens interneurons. Left, the firing precision of the neuron was assessed with slow and fast rates of depolarization induced by current ramps. The voltage slope imposed by the ramp corresponded to the decay of the AHP in the presence or absence of h-channel blocker. Firing became more precise when the rate of depolarization increased (left column, SD = 9.7 ms, 53 trials; right column, SD = 3.7 ms, 46 trials). Right, summary of the data in 3 cells.

that fast rates of membrane depolarization favour temporally precise spiking (Sourdet *et al.* 2003; Cudmore *et al.* 2010). In agreement with this idea, the rate of membrane repolarization during the decay of the AHP was found to be reduced when h-channels were blocked pharmacologically (0.171 ± 0.026 mV ms^{-1} in control *vs.* 0.137 ± 0.023 mV ms^{-1} in Cs^+, $n = 11$, Wilcoxon's test, $P < 0.05$; Fig. 8*B*). To further confirm this hypothesis, the temporal precision of the first spike was analysed in stratum oriens interneurons when firing was elicited by a ramp of current (Fig. 8*C*). The spike jitter was significantly smaller when APs were evoked with a fast rate (SD $= 4.0 \pm 0.3$ ms *vs.* 8.9 ± 1.4 ms, $n = 3$, Wilcoxon's test, $P < 0.05$; Fig. 8*C*). In conclusion, the regularity of the pacemaker activity in stratum oriens interneurons is disorganized when h-channels are blocked through a reduction in the rate of the AHP decay.

EPSP waveform and intrinsic resonance in CA3 pyramidal neurons: role of I_h

h-Channels shape EPSPs and set intrinsic resonance at ~4 Hz in CA1 pyramidal neurons because activation and deactivation time constants of I_h (in the 50–100 ms range) are compatible with EPSP and θ waveforms in these neurons. In CA3 pyramidal neurons, the kinetics of I_h is much slower (Vasilyev & Barish, 2002), suggesting that I_h may not alter intrinsic resonance and EPSP shaping in the same way. We therefore investigated the consequences of the pharmacological blockade of I_h on intrinsic resonance and EPSP waveform in CA3 pyramidal neurons. Intrinsic resonance was assessed in CA3 neurons from acute slices with the injection of a sinusoidal 'chirp' current. In control conditions, the resonance frequency was 1.4 ± 0.3 Hz ($n = 4$; Fig. 9*A*) with a strength (Q value) of 1.65 ± 0.38. In the presence of ZD-7288, input resistance increased to 133.1 ± 2.2% of the control ($n = 4$) and most importantly, the resonance was abolished. The h-dependent resonance frequency in CA3 pyramidal neurons is much lower than that found in CA1 pyramidal neurons (up to 10–12 Hz; Hu *et al.* 2009). Furthermore, the frequency domain of I_h in CA3 pyramidal neurons does not coincide with the power spectrum of EPSPs (usually in the range of 10–40 Hz). One may therefore predict that EPSPs in CA3 neurons will not be affected by h-channel blockers. Connected pairs of CA3 neurons (mean amplitude: 1.5 ± 0.2 mV, $n = 4$) were recorded in hippocampal slice cultures. In the presence of 1 μM ZD-7288 the EPSP duration measured at the baseline was significantly prolonged (from 208 ± 8 ms to 334 ± 28 ms, $n = 4$, Wilcoxon's test, $P < 0.01$). However, the duration of the EPSP at 90% of its amplitude remained virtually unchanged (22 ± 1 *vs.* 23 ± 1 ms in the presence of ZD, $n = 4$, Wilcoxon's test, $P > 0.5$; Fig. 9*B*). To confirm these results obtained in slice cultures, additional experiments were performed in acute slices. As blockade of synaptic inhibition induces epileptiform activity in the CA3 region, EPSPs were simulated by the injection of synaptic-like waveform (see Methods). The amplitude of simulated EPSPs (siEPSPs) was 15 ± 1 mV ($n = 4$). Confirming our previous observations, the duration of siEPSPs at 90% of their amplitude was moderately increased in the presence of 1 μM ZD-7288 (from 19 ± 2 to 25 ± 3 ms, $n = 4$). In fact, the changes observed at CA1 EPSPs were significantly larger than those observed at CA3 EPSPs (changes at CA1 EPSPs in acute slices: $+101 \pm 18$% of the control ($n = 15$), changes at CA3 siEPSPs in acute slices: $+31 \pm 6$% ($n = 4$, Mann–Whitney U test, $P < 0.05$), and at unitary CA3–CA3 EPSPs from organotypic slice cultures: $+3 \pm 4$% ($n = 4$, Mann–Whitney U test, $P < 0.05$)). We conclude that I_h determines intrinsic resonance in CA3 pyramidal neurons but compared to CA1 neurons, I_h has little effect on EPSP waveform in CA3 pyramids.

Blockade of I_h disturbs cortical 3–12 Hz oscillations

We next examined whether h-channels contribute to the organization of rhythmic activity in the hippocampus *in vitro*. As previously reported (Konopacki *et al.* 1987), 50 μM CCh systematically induced robust and non-decrementing θ-like oscillations in CA1 pyramidal neurons recorded in whole-cell configuration from acute slices (Fig. 10*A*, left). In contrast, in the presence of Cs^+ (2.5 mM) or ZD-7288 (1 μM), CCh either failed to induce θ-like oscillations or produced at best decrementing and irregular oscillations (Fig. 10*A*, right). The regularity of the oscillations was assessed by the autocorrelation of the intracellular recording that describes the regularity of single cell oscillation. In the presence of h-channel blockers, the amplitude of the oscillation A_o significantly decreased (from 0.787 ± 0.089, $n = 4$ in control to 0.243 ± 0.089 in the presence of ZD/Cs, $n = 4$, Mann–Whitney U test, $P < 0.05$). A non-significant decrease in the coherence of the oscillation was also observed (the coefficient of oscillation C_o increased from 0.035 ± 0.005 to 0.052 ± 0.014, Mann–Whitney U test, $P < 0.5$). We conclude that h-channels determine the amplitude of hippocampal oscillations in the θ band.

Similar observations were made in slices of rat visual cortex when spontaneous and evoked θ-like oscillations were induced by bath application of CCh (100 μM) and bicuculline (10 μM) (Lukatch & MacIver, 1997). Spontaneous θ-like episodes (duration: 5.9 ± 2.6 s, $n = 7$ slices, frequency: 9.2 ± 2.0 Hz, $n = 7$) recorded extracellularly in layers 4/5 appeared within 5–20 min of CCh application. Simultaneous field-potential and whole-cell recordings from an adjacent L5 pyramidal

neuron showed that field oscillations were correlated with sub- and suprathreshold θ-like activity (Fig. 10*B*, left). In the presence of 1 μM ZD-7288, the duration of the spontaneous θ-like episodes increased (from 5.9 ± 2.6 s in controls and 7.2 ± 3.0 s, $n = 7$ in the presence of ZD-7288, Mann–Whitney U test, $P < 0.05$). Most importantly, the temporal coherence of spontaneous θ-like oscillations was disorganized (Fig. 10*B*, right). Similar changes were observed when θ-like oscillations were evoked by electrical stimulation of the layer II–III (Supplementary Fig. 3*A*)

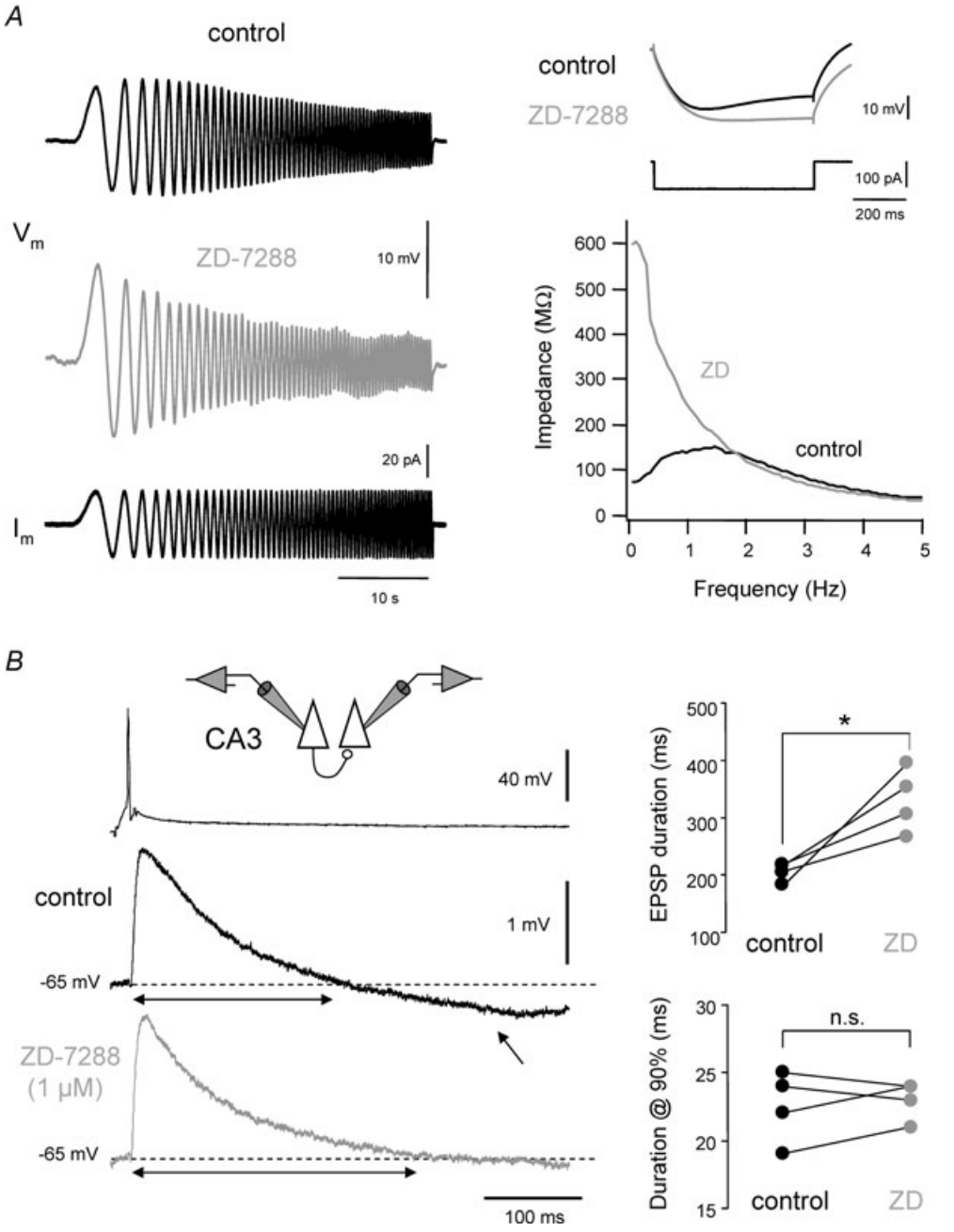

Figure 9. Effects of h-channel blockers on intrinsic resonance and EPSP waveform in CA3 pyramidal neurons
A, intrinsic resonance in CA3 pyramidal neurons from acute hippocampal slices is determined by h-channels. Intrinsic resonance was assessed in CA3 neurons with injection of a sinusoidal 'chirp' current, before and after bath application of 20 μM ZD-7288 (left). Right, effect of ZD-7288 on apparent input resistance (top) and on membrane impedance. Note the lack of resonance in the presence of ZD. *B*, waveform of unitary CA3–CA3 EPSPs from organotypic slice cultures was analysed. EPSP duration at the baseline level is increased but not near the peak of the EPSP. Right, plots of EPSP duration measured at the baseline (top) or at 90% of its amplitude.

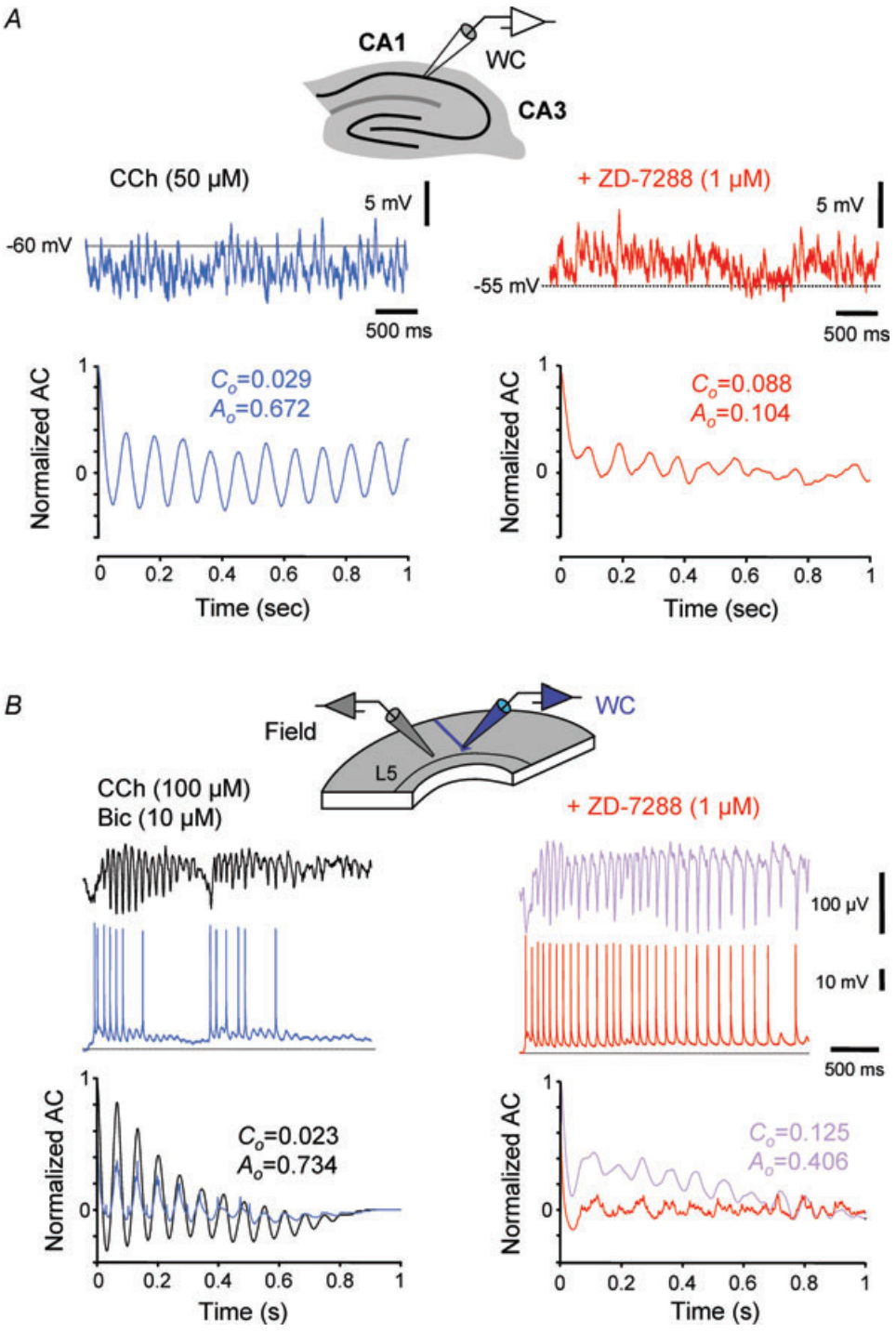

Figure 10. Effects of h-channel blocker on hippocampal and neocortical θ-oscillations *in vitro*
A, spontaneous oscillations induced by 50 μM carbachol (CCh) and recorded in a CA1 pyramidal neuron (top left). Lower left graph, auto-correlation function of the membrane potential. Note the regularity of oscillation with very small attenuation in the amplitude over >10 cycles. Top right, CCh evoked oscillations in the presence of 1 μM ZD-7288. Note the pronounced attenuation in the oscillation amplitude after a few cycles in the auto-correlation function. *B*, disorganization of visual cortical θ-oscillation *in vitro* by pharmacological blockade of I_h. Left, spontaneous θ oscillations induced by 50 μM CCh and 10 μM bicuculline (Bic) recorded simultaneously in field potential (black trace) and from a L5 pyramidal neuron (blue trace) in the visual cortex. Lower graph, auto-correlation function of the extracellular (black) and intracellular (blue) signals. Right, in the presence of the h-channel blocker ZD-7288, the coherence and amplitude of extracellular and intracellular oscillations decreased. Note the increased number of spikes per θ episode (control: 13 spikes/episode, ZD-7288: 29 spikes/episode).

and data were pooled together. In the presence of ZD-7288, the coefficient of oscillation C_o increased from 0.08 ± 0.01 in controls to 0.14 ± 0.02 (Mann–Whitney U test, $P < 0.05$) and the amplitude of oscillation A_o dropped from 0.902 ± 0.047 in controls to 0.722 ± 0.064, $n = 5$ in the presence of ZD-7288 (Mann–Whitney U test, $P < 0.05$; Supplementary Fig. 3*B*). In conclusion, h-channels participate in the temporal organization of hippocampal and neocortical network activity in the θ-frequency range.

Discussion

We show here that, in addition to their well-known action on intrinsic resonance and pacemaker spiking activity, h-channels also determine the temporal precision of EPSP–spike and IPSP–spike coupling in CA1 pyramidal neurons (Fig. 11*A*). In fact, I_h sharpens EPSPs and IPSPs, thereby reducing the temporal jitter of evoked and rebound spikes. All these features may act in synergy among different cell types to set the regularity of oscillations at the network level (Fig. 11*B*). Finally, our data also indicate that the selective pharmacological blockade of postsynaptic h-current reduces the coherence and the amplitude of hippocampal and neocortical oscillations *in vitro*.

h-Channels and intrinsic resonance

It is well established that h-channels contribute significantly to intrinsic membrane resonance in the theta range in both L5 and CA1 pyramidal neurons (Hu *et al.* 2002; Ulrich, 2002; Narayanan & Johnston, 2008; Hu *et al.* 2009). h-Current is also present postsynaptically in a wide range of GABAergic hippocampal interneurons (Maccaferri & McBain, 1996; Lupica *et al.* 2001; Aponte *et al.* 2006). We focused our study on stratum oriens interneurons because their prominent h-current (Maccaferri & McBain, 1996; Lupica *et al.* 2001) and their sensitivity to muscarinic receptor stimulation (Lawrence *et al.* 2006) make them putative candidates for the patterning of CCh-dependent θ oscillations. We show that stratum oriens interneurons display a resonance frequency at 2–3 Hz that linearly depends on membrane potential. The resonance frequency was found to be faster at -75 mV than at -55 mV. Importantly, we show that h-channels play a critical role in the resonance of stratum oriens interneurons as reported previously (Storm & Hu, 2003). In the presence of external Cs^+, resonance was totally abolished and the impedance profile resembled that of a purely passive membrane (Hutcheon & Yarom, 2000). Thus, h-channels not only determine the resonance frequency in the lower θ-frequency range in L5 and CA1 pyramidal neurons but also in stratum oriens interneurons.

I_h was also found to determine intrinsic resonance at 1–2 Hz in CA3 pyramidal neurons. Compared to the 4 Hz resonance found in CA1 pyramidal cells (Hu *et al.* 2002), this value is much lower. Two reasons may account for this difference. Compared to CA1 cells, CA3 pyramidal neurons display a longer membrane time constant (Schwartzkroin, 1977; Johnston, 1980) and slower kinetics of I_h (Vasilyev & Barish, 2002).

I_h sets the temporal precision of EPSP–spike coupling

We show that blocking I_h with external Cs^+ or ZD-7288 increased the jitter of spikes evoked by just supra-threshold EPSPs in CA1 pyramidal neurons whereas addition of h-conductance with the dynamic-clamp technique reduced this jitter. In these latter experiments the h-conductance was injected in the soma. Although h-channels in CA1 pyramidal neurons are mostly located in the dendrites, we believe that this experiment is conclusive. In fact, the critical point here is the shaping of the EPSP in the cell body and ultimately at the site of spike generation (i.e. the axon initial segment). Although additional experiments are required to specifically address this issue, slow signals like EPSPs are generally transferred from the cell body to the proximal region of the axon without any major distortion (Shu *et al.* 2006; Debanne *et al.* 2011).

The duration of the EPSP at 90% of its maximal amplitude was significantly prolonged in the presence of h-channel blocker. Interestingly, the effects of Cs^+ and ZD-7288 on EPSP duration and precision were correlated, indicating that EPSP–spike precision depends on the shape of the EPSP at its maximum. Importantly, the ZD-7288-sensitive outward virtual current evoked by a voltage command mimicking an EPSP coincides temporally with its falling phase (i.e. after the window for spike generation). Our study therefore confirms the definition of a simple rule governing the precision of EPSP–spike coupling where precision is improved when the outward current (here due to the deactivation of I_h) follows the inward current. Thus, I_h represents the fourth example of ionic current (following Kv channels in interneurons (Fricker & Miles, 2000), $GABA_A$ receptor in CA1 pyramidal neurons (Pouille & Scanziani, 2001) and Nav in CA1 pyramidal neurons (Vervaeke *et al.* 2006)) that determines EPSP–spike precision. In addition, it has been shown that the fast membrane kinetics or synaptic currents encountered in adult neurons also improve EPSP–spike precision (Cathala *et al.* 2003). The finding that I_h enhances temporal precision of spikes evoked by EPSPs may certainly be generalized to all neurons that express this current with kinetics of deactivation that are compatible with the duration of incoming EPSPs, such as oriens interneurons or L5 pyramidal cells. However, it might not be

the case in CA3 neurons because I_h has little effect on EPSP shaping in these neurons. The lack of effect of ZD-7288 on EPSP waveform at unitary CA3–CA3 connections in hippocampal slice culture is unlikely to result from specific characteristics of h-channels in this preparation. Indeed, the increase in input resistance obtained in CA3 neurons from slices and from slice cultures was comparable (133% and 143%, respectively). Moreover, EPSPs simulated by synaptic-like current injected in CA3 pyramidal neurons in acute slices were also weakly affected by the blockade of h-channels. Rather, the moderate effect of h-channel blockers on EPSP waveform can be easily explained by the relatively small conductance and the slow kinetics of I_h in these neurons (Vasilyev & Barish, 2002).

The role of I_h in EPSP–spike coupling has been assessed in this study under the pharmacological blockade of $GABA_A$ receptor-mediated inhibition. In physiological conditions, the contribution of I_h might be significantly smaller, since the time course of evoked EPSPs is generally determined by di-synaptic inhibition (Fricker & Miles, 2000; Pouille & Scanziani, 2001). However, the recent study by Pavlov and co-workers indicates that the depolarizing action of I_h enhances temporal precision of neuronal integration because it maintains a voltage gradient for fast hyperpolarizing GABAergic transmission (Pavlov *et al.* 2011).

I_h improves IPSP–spike precision and pacemaker activity via voltage speeding up

Basket cells synchronize firing of pyramidal cell populations through IPSP-mediated rebound spike firing (Cobb *et al.* 1995). What is the contribution of I_h in this process? We show that I_h determines the precision of IPSP–spike coupling at inhibitory synapses between putative basket cells and CA1 pyramidal neurons. The temporal dispersion of rebound spikes evoked by mono-synaptic IPSPs was enhanced in the presence of ZD-7288 or external Cs^+. Interestingly, the IPSP decay slope was significantly reduced by h-channel blockers because the activation of I_h by the hyperpolarization produced by the IPSP was suppressed. Thus, the loss of temporal precision might be attributed to a reduction in the rate of membrane

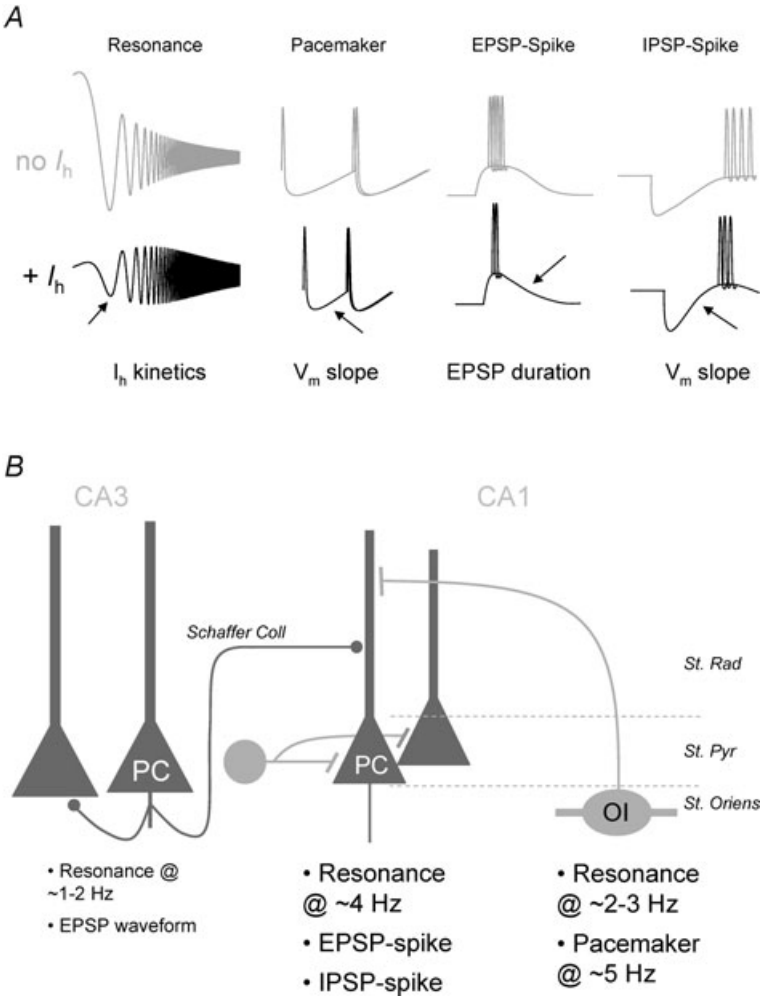

Figure 11. Action of I_h on the temporal organization of neuronal activity in the hippocampus
A, summary of the effects of I_h in cortical neurons. *B*, simplified scheme of the hippocampus (PC: pyramidal cell; OI: stratum oriens interneuron). In CA1 pyramidal neurons, I_h has 3 main actions (intrinsic resonance at ~4 Hz, EPSP–spike precision and IPSP–spike precision). In OI, h-channels determine intrinsic resonance at ~3 Hz and the regularity of pacemaker activity at ~5 Hz. In CA3 pyramidal neurons, I_h determines intrinsic resonance at ~1–2 Hz and EPSP waveform. But compared to CA1 pyramidal neurons, this contribution is smaller in CA3 pyramids.

depolarization before spike generation (Sourdet *et al.* 2003; Cudmore *et al.* 2010). Furthermore, simultaneous recordings from pairs of CA1 pyramidal neurons showed that synchronous firing was reduced when h-channels were blocked pharmacologically. Thus, our data indicate that basket cells promote network synchronization through the h-channel-dependent shaping of IPSPs in CA1 region.

We confirmed here that pharmacological blockade of h-channels disturbed pacemaker activity in oriens interneurons (Maccaferri & McBain, 1996; Gillies *et al.* 2002). In these studies, the mechanism underlying the decreased regularity of firing was, however, not clearly identified. We show in our study that the rate of AHP repolarization is significantly reduced in the presence of h-channel blockers. Importantly, the temporal jitter of APs evoked by a ramp was reduced when the rate of depolarization was moderately increased in oriens interneurons (Fig. 8). This conclusion may also well apply to principal neurons. In fact, the genetic deletion of HCN1 enlarges the AHP and alters the pattern of spike firing in pyramidal cells of the entorhinal cortex (Nolan *et al.* 2007). The mechanism that governs slope-dependent precision is not fully elucidates but it could be related to the fact that spike threshold is not a fixed point but rather a voltage range because of stochastic properties of ion channels (Schneidman *et al.* 1998; White *et al.* 2000). Fast rates of depolarization before spike generation represent a favourable condition for temporally precise firing probably because the time window during which voltage-gated channel noise may blur action potential generation is minimized (L.P. Savtchenko, P. Deglise, M. Russier, N. Ankri & D. Debanne unpublished observations).

Implications for network activity: oscillations and hyper-synchrony

Our data indicate that oscillatory activity is profoundly disturbed in the hippocampus and in the visual cortex following pharmacological blockade of h-channels. In contrast, Nolan and co-workers (2004) reported that the power of theta oscillations was augmented in HCN1 knockout mice. This discrepancy may result from compensatory regulation of synaptic transmission and intrinsic excitability caused by genetic silencing of voltage-gated ion channels (Turrigiano & Nelson, 2004). In fact, a recent study shows that the lack of HCN1 subunit in $HCN^{-/-}$ mice is compensated by the up-regulation of $GABA_A$ receptor-mediated inhibition (Chen *et al.* 2010). Another explanation may result from interspecies differences. The magnitude of h-current and intrinsic resonance is smaller in mice compared to rats (Routh *et al.* 2009).

In the visual cortex, the oscillations were prolonged in the presence of ZD-7288. This is not totally surprising since the blockade of h-channels essentially prolongs EPSP duration and promotes late spiking (Fig. 3).

The I_h-dependent synchronization of network activity will have several important functional consequences. First, the developmental up-regulation of the h-channel (Vasilyev & Barish, 2002) may be at the origin of the increased coherence of brain oscillations reported during postnatal development in rat (Konopacki *et al.* 1988). In addition, activity-dependent plasticity of h-channel activity could produce associated changes in network synchronization. In fact, I_h is homeostatically up-regulated by high levels of synaptic activity (van Welie *et al.* 2004), postsynaptic depolarization (van Welie *et al.* 2004; Fan *et al.* 2005; Narayanan & Johnston, 2007; Campanac *et al.* 2008) or hyperthermia-induced epilepsy (Chen *et al.* 2001). Our study suggests that homeostatic increase in I_h may represent a suitable mechanism to increase network synchrony. The susceptibility to seizure is enhanced (Chen *et al.* 2001) and dendritic resonance is facilitated (Narayanan & Johnston, 2007) when h-channel activity is homeostatically up regulated, indicating that network hyper-synchrony may constitute a perverse consequence of this regulation. Our results are also compatible with the loss of θ oscillations observed in the kainic acid model of epilepsy in which I_h is reduced (Dugladze *et al.* 2007).

Conclusion: towards definitions of simple rules governing temporal spike precision

Despite the variety of neuronal operations controlled by I_h, its contribution in the temporal organization of neuronal activity might be summarized in three main rules. I_h (1) sets subthreshold resonance in pyramidal cells and interneurons, (2) enhances EPSP–spike precision by reducing EPSP duration, thus limiting the time during which an AP can be elicited, and (3) accelerates the rate of depolarization during the decay of AHPs or IPSPs. All these elementary operations contribute together to lock slow frequency oscillations in the theta range in hippocampal and neocortical circuits.

References

Aponte Y, Lien CC, Reisinger E & Jonas P (2006). Hyperpolarization-activated cation channels in fast-spiking interneurons of rat hippocampus. *J Physiol* **574**, 229–243.

Axmacher N & Miles R (2004). Intrinsic cellular currents and the temporal precision of EPSP-action potential coupling in CA1 pyramidal cells. *J Physiol* **555**, 713–725.

Bal T & McCormick DA (1996). What stops synchronized thalamocortical oscillations? *Neuron* **17**, 297–308.

Bender RA, Galindo R, Mameli M, Gonzalez-Vega R, Valenzuela CF & Baram TZ (2005). Synchronized network activity in developing rat hippocampus involves regional hyperpolarization-activated cyclic nucleotide-gated (HCN) channel function. *Eur J Neurosci* **22**, 2669–2674.

Biel M, Wahl-Schott C, Michalakis S & Zong X (2009). Hyperpolarization-activated cation channels: from genes to function. *Physiol Rev* **89**, 847–885.

Boudkkazi S, Carlier E, Ankri N, Caillard O, Giraud P, Fronzaroli-Molinieres L & Debanne D (2007). Release-dependent variations in synaptic latency: a putative code for short- and long-term synaptic dynamics. *Neuron* **56**, 1048–1060.

Boudkkazi S, Fronzaroli-Molinieres L & Debanne D (2011). Presynaptic action potential waveform determines cortical synaptic latency. *J Physiol* **589**, 1117–1131.

Bringuier V, Fregnac Y, Baranyi A, Debanne D & Shulz DE (1997). Synaptic origin and stimulus dependency of neuronal oscillatory activity in the primary visual cortex of the cat. *J Physiol* **500**, 751–774.

Campanac E, Daoudal G, Ankri N & Debanne D (2008). Downregulation of dendritic I_h in CA1 pyramidal neurons after LTP. *J Neurosci* **28**, 8635–8643.

Carlier E, Sourdet V, Boudkkazi S, Deglise P, Ankri N, Fronzaroli-Molinieres L & Debanne D (2006). Metabotropic glutamate receptor subtype 1 regulates sodium currents in rat neocortical pyramidal neurons. *J Physiol* **577**, 141–154.

Castro-Alamancos MA, Rigas P & Tawara-Hirata Y (2007). Resonance (approximately 10 Hz) of excitatory networks in motor cortex: effects of voltage-dependent ion channel blockers. *J Physiol* **578**, 173–191.

Cathala L, Brickley S, Cull-Candy S & Farrant M (2003). Maturation of EPSCs and intrinsic membrane properties enhances precision at a cerebellar synapse. *J Neurosci* **23**, 6074–6085.

Chapman CA & Lacaille JC (1999). Intrinsic theta-frequency membrane potential oscillations in hippocampal CA1 interneurons of stratum lacunosum-moleculare. *J Neurophysiol* **81**, 1296–1307.

Chen K, Aradi I, Thon N, Eghbal-Ahmadi M, Baram TZ & Soltesz I (2001). Persistently modified h-channels after complex febrile seizures convert the seizure-induced enhancement of inhibition to hyperexcitability. *Nat Med* **7**, 331–337.

Chen X, Shu S, Schwartz LC, Sun C, Kapur J & Bayliss DA (2010). Homeostatic regulation of synaptic excitability: tonic $GABA_A$ receptor currents replace I_h in cortical pyramidal neurons of HCN1 knock-out mice. *J Neurosci* **30**, 2611–2622.

Chevaleyre V & Castillo PE (2002). Assessing the role of I_h channels in synaptic transmission and mossy fibre LTP. *Proc Natl Acad Sci U S A* **99**, 9538–9543.

Cobb SR, Buhl EH, Halasy K, Paulsen O & Somogyi P (1995). Synchronization of neuronal activity in hippocampus by individual GABAergic interneurons. *Nature* **378**, 75–78.

Cobb SR, Larkman PM, Bulters DO, Oliver L, Gill CH & Davies CH (2003). Activation of I_h is necessary for patterning of mGluR and mAChR induced network activity in the hippocampal CA3 region. *Neuropharmacology* **44**, 293–303.

Cudmore RH, Fronzaroli-Molinieres L, Giraud P & Debanne D (2010). Spike-time precision and network synchrony are controlled by the homeostatic regulation of the D-type potassium current. *J Neurosci* **30**, 12885–12895.

Debanne D, Boudkkazi S, Campanac E, Cudmore RH, Giraud P, Fronzaroli-Molinieres L, Carlier E & Caillard O (2008). Paired-recordings from synaptically coupled cortical and hippocampal neurons in acute and cultured brain slices. *Nat Protoc* **3**, 1559–1568.

Debanne D, Campanac E, Bialowas A, Carlier E & Alcaraz G (2011). Axon physiology. *Physiol Rev* **91**, 555–602.

Dickson CT, Magistretti J, Shalinsky MH, Fransen E, Hasselmo ME & Alonso A (2000) Properties and role of I_h in the pacing of subthreshold oscillations in entorhinal cortex layer II neurons. *J Neurophysiol* **83**, 2562–2579.

Drummond GB (2009) Reporting ethical matters in *The Journal of Physiology*: standards and advice. *J Physiol* **587**, 713–719.

Dugladze T, Vida I, Tort AB, Gross A, Otahal J, Heinemann U, Kopell NJ & Gloveli T (2007). Impaired hippocampal rhythmogenesis in a mouse model of mesial temporal lobe epilepsy. *Proc Natl Acad Sci U S A* **104**, 17530–17535.

Fan Y, Fricker D, Brager DH, Chen X, Lu HC, Chitwood RA & Johnston D (2005). Activity-dependent decrease of excitability in rat hippocampal neurons through increases in I_h. *Nat Neurosci* **8**, 1542–1551.

Fricker D & Miles R (2000). EPSP amplification and the precision of spike timing in hippocampal neurons. *Neuron* **28**, 559–569.

Gillies MJ, Traub RD, LeBeau FE, Davies CH, Gloveli T, Buhl EH & Whittington MA (2002). A model of atropine-resistant theta oscillations in rat hippocampal area CA1. *J Physiol* **543**, 779–793.

Griguoli M, Maul A, Nguyen C, Giorgetti A, Carloni P & Cherubini E (2010). Nicotine blocks the hyperpolarization-activated current I_h and severely impairs the oscillatory behaviour of oriens-lacunosum moleculare interneurons. *J Neurosci* **30**, 10773–10783.

Gu N, Vervaeke K, Hu H & Storm JF (2005). Kv7/KCNQ/M and HCN/h, but not KCa2/SK channels, contribute to the somatic medium after-hyperpolarization and excitability control in CA1 hippocampal pyramidal cells. *J Physiol* **566**, 689–715.

Haas JS, Dorval AD 2nd & White JA (2007). Contributions of I_h to feature selectivity in layer II stellate cells of the entorhinal cortex. *J Comput Neurosci* **22**, 161–171.

Hu H, Vervaeke K, Graham LJ & Storm JF (2009) Complementary theta resonance filtering by two spatially segregated mechanisms in CA1 hippocampal pyramidal neurons. *J Neurosci* **29**, 14472–14483.

Hu H, Vervaeke K & Storm JF (2002). Two forms of electrical resonance at theta frequencies, generated by M-current, h-current and persistent Na^+ current in rat hippocampal pyramidal cells. *J Physiol* **545**, 783–805.

Huang CW, Huang CC, Liu YC & Wu SN (2004). Inhibitory effect of lamotrigine on A-type potassium current in hippocampal neuron-derived H19-7 cells. *Epilepsia* **45**, 729–736.

Hutcheon B, Miura RM & Puil E (1996). Subthreshold membrane resonance in neocortical neurons. *J Neurophysiol* **76**, 683–697.

Hutcheon B & Yarom Y. (2000) Resonance, oscillation and the intrinsic frequency preferences of neurons. *Trends Neurosci* **23**, 216–222.

Johnston D (1980). Passive cable properties of hippocampal CA3 pyramidal neurons. *Cell Mol Neurobiol* **1**, 41–55.

Kitayama M, Taguchi T, Miyata H, Matsuda Y, Yamauchi T & Kogure S (2002). The extracellular current blocking effect of cesium chloride on the theta wave in the rabbit hippocampal CA1 region. *Neurosci Lett* **334**, 45–48.

Klausberger T & Somogyi P (2008). Neuronal diversity and temporal dynamics: the unity of hippocampal circuit operations. *Science* **321**, 53–57.

Konopacki J, Bland BH & Roth SH (1988). The development of carbachol-induced EEG 'theta' examined in hippocampal formation slices. *Brain Res* **466**, 229–232.

Konopacki J, MacIver MB, Bland BH & Roth SH (1987). Carbachol-induced EEG 'theta' activity in hippocampal brain slices. *Brain Res* **405**, 196–198.

Lawrence JJ (2008). Cholinergic control of GABA release: emerging parallels between neocortex and hippocampus. *Trends Neurosci* **31**, 317–327.

Lawrence JJ, Statland JM, Grinspan ZM & McBain CJ (2006). Cell type-specific dependence of muscarinic signalling in mouse hippocampal stratum oriens interneurones. *J Physiol* **570**, 595–610.

Lorincz A, Notomi T, Tamas G, Shigemoto R & Nusser Z (2002). Polarized and compartment-dependent distribution of HCN1 in pyramidal cell dendrites. *Nat Neurosci* **5**, 1185–1193.

Lukatch HS & MacIver MB (1997). Physiology, pharmacology, and topography of cholinergic neocortical oscillations in vitro. *J Neurophysiol* **77**, 2427–2445.

Lupica CR, Bell JA, Hoffman AF & Watson PL (2001). Contribution of the hyperpolarization-activated current (I_h) to membrane potential and GABA release in hippocampal interneurons. *J Neurophysiol* **86**, 261–268.

Luthi A & McCormick DA (1998). H-current: properties of a neuronal and network pacemaker. *Neuron* **21**, 9–12.

Maccaferri G, Mangoni M, Lazzari A & DiFrancesco D (1993). Properties of the hyperpolarization-activated current in rat hippocampal CA1 pyramidal cells. *J Neurophysiol* **69**, 2129–2136.

Maccaferri G & McBain CJ (1996). The hyperpolarization-activated current (I_h) and its contribution to pacemaker activity in rat CA1 hippocampal stratum oriens-alveus interneurones. *J Physiol* **497**, 119–130.

Magee JC (1998). Dendritic hyperpolarization-activated currents modify the integrative properties of hippocampal CA1 pyramidal neurons. *J Neurosci* **18**, 7613–7624.

Narayanan R & Johnston D (2007). Long-term potentiation in rat hippocampal neurons is accompanied by spatially widespread changes in intrinsic oscillatory dynamics and excitability. *Neuron* **56**, 1061–1075.

Narayanan R & Johnston D (2008). The h channel mediates location dependence and plasticity of intrinsic phase response in rat hippocampal neurons. *J Neurosci* **28**, 5846–5860.

Nolan MF, Dudman JT, Dodson PD & Santoro B (2007). HCN1 channels control resting and active integrative properties of stellate cells from layer II of the entorhinal cortex. *J Neurosci* **27**, 12440–12451.

Nolan MF, Malleret G, Dudman JT, Buhl DL, Santoro B, Gibbs E, Vronskaya S, Buzsaki G, Siegelbaum SA, Kandel ER & Morozov A (2004). A behavioural role for dendritic integration: HCN1 channels constrain spatial memory and plasticity at inputs to distal dendrites of CA1 pyramidal neurons. *Cell* **119**, 719–732.

Orban G, Kiss T & Erdi P (2006). Intrinsic and synaptic mechanisms determining the timing of neuron population activity during hippocampal theta oscillation. *J Neurophysiol* **96**, 2889–2904.

Pape HC (1996). Queer current and pacemaker: the hyperpolarization-activated cation current in neurons. *Annu Rev Physiol* **58**, 299–327.

Pavlov I, Scimemi A, Savtchenko L, Kullmann DM & Walker MC (2011). I_h-mediated depolarization enhances the temporal precision of neuronal integration. *Nat Commun* **2**, 199.

Pike FG, Goddard RS, Suckling JM, Ganter P, Kasthuri N & Paulsen O (2000). Distinct frequency preferences of different types of rat hippocampal neurones in response to oscillatory input currents. *J Physiol* **529**, 205–213.

Poolos NP, Migliore M & Johnston D (2002). Pharmacological upregulation of h-channels reduces the excitability of pyramidal neuron dendrites. *Nat Neurosci* **5**, 767–774.

Pouille F & Scanziani M (2001). Enforcement of temporal fidelity in pyramidal cells by somatic feed-forward inhibition. *Science* **293**, 1159–1163.

Prinz AA, Abbott LF & Marder E (2004). The dynamic clamp comes of age. *Trends Neurosci* **27**, 218–224.

Rateau Y & Ropert N (2006). Expression of a functional hyperpolarization-activated current (I_h) in the mouse nucleus reticularis thalami. *J Neurophysiol* **95**, 3073–3085.

Remy S, Urban BW, Elger CE & Beck H (2003). Anticonvulsant pharmacology of voltage-gated Na^+ channels in hippocampal neurons of control and chronically epileptic rats. *Eur J Neurosci* **17**, 2648–2658.

Robinson RB & Siegelbaum SA (2003). Hyperpolarization-activated cation currents: from molecules to physiological function. *Annu Rev Physiol* **65**, 453–480.

Rotstein HG, Pervouchine DD, Acker CD, Gillies MJ, White JA, Buhl EH, Whittington MA & Kopell N (2005). Slow and fast inhibition and an H-current interact to create a theta rhythm in a model of CA1 interneuron network. *J Neurophysiol* **94**, 1509–1518.

Routh BN, Johnston D, Harris K & Chitwood RA (2009). Anatomical and electrophysiological comparison of CA1 pyramidal neurons of the rat and mouse. *J Neurophysiol* **102**, 2288–2302.

Saviane C, Mohajerani MH & Cherubini E (2003). An ID-like current that is downregulated by Ca^{2+} modulates information coding at CA3–CA3 synapses in the rat hippocampus. *J Physiol* **552**, 513–524.

Schneidman E, Freedman B & Segev I (1998). Ion channel stochasticity may be critical in determining the reliability and precision of spike timing. *Neural Comput* **10**, 1679–1703.

Schwartzkroin PA (1977). Further characteristics of hippocampal CA1 cells in vitro. *Brain Res* **128**, 53–68.
Sharp AA, O'Neil MB, Abbott LF & Marder E (1993). The dynamic clamp: artificial conductances in biological neurons. *Trends Neurosci* **16**, 389–394.
Shu Y, Hasenstaub A, Duque A, Yu Y & McCormick DA (2006). Modulation of intracortical synaptic potentials by presynaptic somatic membrane potential. *Nature* **441**, 761–765.
Soleng AF, Chiu K & Raastad M (2003). Unmyelinated axons in the rat hippocampus hyperpolarize and activate an H current when spike frequency exceeds 1 Hz. *J Physiol* **552**, 459–470.
Sourdet V, Russier M, Daoudal G, Ankri N & Debanne D (2003). Long-term enhancement of neuronal excitability and temporal fidelity mediated by metabotropic glutamate receptor subtype 5. *J Neurosci* **23**, 10238–10248.
Stoppini L, Buchs PA & Muller D (1991). A simple method for organotypic cultures of nervous tissue. *J Neurosci Methods* **37**, 173–182.
Storm JF (1989). An after-hyperpolarization of medium duration in rat hippocampal pyramidal cells. *J Physiol* **409**, 171–190.
Storm JF & Hu H (2003). Theta-resonance generated by H and M-channels in hippocampal stratum oriens interneurons. *2003 Abstract Viewer/Itinerary Planner*, Programme No. 258.7. Society for Neuroscience, Washington, DC.
Traub RD, Miles R & Wong RK (1989). Model of the origin of rhythmic population oscillations in the hippocampal slice. *Science* **243**, 1319–1325.
Turrigiano GG & Nelson SB (2004). Homeostatic plasticity in the developing nervous system. *Nat Rev Neurosci* **5**, 97–107.
Ulrich D (2002). Dendritic resonance in rat neocortical pyramidal cells. *J Neurophysiol* **87**, 2753–2759.
van Brederode JF & Spain WJ (1995). Differences in inhibitory synaptic input between layer II–III and layer V neurons of the cat neocortex. *J Neurophysiol* **74**, 1149–1166.
van Welie I, van Hooft JA & Wadman WJ (2004). Homeostatic scaling of neuronal excitability by synaptic modulation of somatic hyperpolarization-activated I_h channels. *Proc Natl Acad Sci U S A* **101**, 5123–5128.
Vasilyev DV & Barish ME (2002). Postnatal development of the hyperpolarization-activated excitatory current I_h in mouse hippocampal pyramidal neurons. *J Neurosci* **22**, 8992–9004.
Vervaeke K, Hu H, Graham LJ & Storm JF (2006). Contrasting effects of the persistent Na^+ current on neuronal excitability and spike timing. *Neuron* **49**, 257–270.
White JA, Rubinstein JT & Kay AR (2000). Channel noise in neurons. *Trends Neurosci* **23**, 131–137.

Author contributions

Conception and design of the experiments: P.G., Em.C. and D.D. Collection, analysis and interpretation of data: P.G., Em.C., C.G., A.B., R.H.C, Ed.C., L.F.M. and D.D. Drafting the manuscript: P.G., Em.C. and D.D. The experiments were performed in the laboratory of D.D. at INSERM U641, Marseille, France. All authors approved the final version of the manuscript.

Acknowledgements

We thank Drs Jan Behrens, Andreas Lüthi, Nicole Ropert and Michael Seagar for constructive criticisms on the manuscript. We thank P. Giraud for help with hippocampal slice cultures, and C. Gomez-Fuentes and M. Buisine for excellent technical assistance. This work was supported by INSERM, CNRS, Agence Nationale de la Recherche (ANR-06-Neuro-014-01 to D.D.), Région PACA (APO 'Plexin' to D.D.), FRM (doctoral grants to P.G. and Em.C.), IBRO-INSERM (post-doctoral fellowship to R.H.C.), AFM (post-doctoral fellowship to R.H.C.), and the Ministry of Research (doctoral grants to P.G., Em.C., A.B. and C.G.).